Creep of Aluminum (Rich) - Nickel Eutectic

by

Donald D. Himbeault

A thesis
presented to the University of Manitoba
in partial fulfillment of the
requirements for the degree of
Master of Science
in
Mechanical Engineering

Winnipeg, Manitoba

CREEP OF ALUMINUM (RICH) - NICKEL EUTECTIC

BY

DONALD D. HIMBEAULT

A thesis submitted to the Faculty of Graduate Studies of
the University of Manitoba in partial fulfillment of the requirements
of the degree of

MASTER OF SCIENCE

ABSTRACT

Specimens of Al-Al_3Ni eutectic, directionally solidified at 8 cm per hour, were creep tested under a number of different stress and temperature conditions to characterize the creep behavior of the composite. It was found that when the creep results are described by the conventional creep equation,

$$\dot{\epsilon} kT = A_1 D_0 Gb (\sigma)^n \exp(-Q/RT)$$

four regions of creep behavior were observed. A deformation map was plotted to show pictorially these different regions, which could possibly correspond to the four creep regions in pure aluminum; Coble, Nabarro-Herring, high temperature climb and low temperature climb. In one region the stress exponent was 2.4 and the activation energy for creep was close to that for grain boundary diffusion of aluminum, typical of diffusional or Coble creep of aluminum. In the other regions the stress exponent and/or the activation energy for creep were usually higher than that for the dislocation creep for aluminum and lower then that for creep in the fiber phase. Thus, no identifiable mechanism for creep could be attributed to these other three regions in terms of single phase parameters.

A method of rationalizing the strong stress and temperature dependence of the creep rate of two phase materials is to consider the presence of a threshold stress, σ_0, which opposes the action of the applied stress. The stress and temperature dependence of the steady state creep rate can be described as

$$\dot{\epsilon} kT = A_2 D_0 Gb (\sigma-\sigma_0)^{n_0} \exp(-Q^* /RT)$$

where σ_0 is determined by stress change experiments. Three regions of creep behavior could now be discerned characterized by stress exponent values of 2.4, 2.1 and 4.8 and with activation energies for creep of 70, 51.6 and 116 kJ/mole respectively. The first set of values is in accordance with a model for diffusional creep. The second set of values indicates a dislocation creep model controlled by dislocation climb at interphase boundaries of two phase materials. The last set is representative of dislocation creep of aluminum where the activation energy for creep is that of self diffusion of aluminum. A second deformation map for these regions is plotted.

The creep behavior observed in the composite is in accordance with models for creep in aligned composites where enhanced matrix flow at the fiber ends is the major source of deformation in the overall creep of the composite. It thus appears that creep of the aluminum phase is rate controlling in the creep of the Al-Ni composite.

ACKNOWLEDGMENTS

I would like to thank Dr. J.R.Cahoon for his encouragement and advice during the course of this research. The assistance of the technical staff of the metallurgical group and of the mechanical engineering machine shop was also greatly appreciated.

The author is grateful to the Aluminum Company of Canada who supplied the aluminum and the International Nickel Company who supplied the nickel. The assistance of Dr.J. Shewchuk in using the creep machines is also gratefully acknowledged.

This research was funded by an operating grant from the Natural Science and Engineering Research Council of Canada.

CONTENTS

LIST OF TABLES

LIST OF FIGURES

INTRODUCTION

GENERAL

Considerable effort is being made to improve the high temperature performance of certain critical components such as turbine blades in order to increase the efficiency of gas turbine engines, particularly in aircraft propulsion. Improvements have been made through a combination of alloying and processing with directional solidification being an important stage in the production of components where either columnar grained or single crystal superalloys are required. As well, directional solidification of eutectic alloys has been shown to produce aligned composite microstructures which show good fiber reinforcement even at high temperatures[1,2]. However, the technology of directionally solidified materials has been implemented so rapidly that the creep behavior of these materials is not fully understood when attempting to describe their high temperature deformation in terms of the creep parameters used for single phase materials. Reported values of the activation energy and the stress exponent for creep of aligned composites are, in general, substantially larger than the values for the metal matrix alone [1,3,4].

A method of rationalizing the strong dependence of the creep rate on stress and temperature of aligned composites is to consider that the creep deformation takes place under an effective stress $(\sigma-\sigma_0)$, where σ_0 is a threshold stress, and not under the full effect of the applied stress, σ. When the threshold stress is taken into account, the activation energy for creep becomes that of self diffusion for the matrix and the stress exponent is in the range of 3-5 which is that accepted for creep controlled by dislocation climb mechanisms.

OBJECTIVES OF RESEARCH WORK

The chief aim of this work is to study the creep behavior of a directionally solidified eutectic composite grown at a single speed to determine the contribution of each phase in the creep properties of the alloy. Stress decrement experiments were performed to find the value of the threshold stress and to determine the significance of σ_0 in describing the creep of the composite. Deformation maps have also been plotted for the composite and proposals are forwarded concerning the creep mechanisms occuring in the composite in the various stress and temperature fields.

LITERATURE SURVEY

INTRODUCTION

In the 1960's and early 1970's, much work was done in the area of controlled unidirectional solidification of binary eutectic alloys . By this process of solidification it was possible to produce structures consisting of two phases in the form of strong aligned whiskers or lamellae reinforcing a continuous metal matrix. The degree of fiber reinforcement the composite receives by this process depends on the strength and volume fraction of the reinforcing phase and on the coherency of the bond between the reinforcing phase and the matrix. One material which has shown good reinforcing behavior is the Al-6.2 wt.% Ni eutectic as demonstrated by Lemkey, et al[5]. When directionally solidified it was found that the alloy's stength in the solidification direction increased threefold over its strength in the random, as cast condition.

The 6.2 wt.% Ni eutectic was chosen here as the alloy to be studied in characterizing the creep of composite materials since it shows good reinforcing properties and considerable solidification information is readily available in the literature.

DIRECTIONAL SOLIDIFICATION

In conventional casting, an alloy melt is poured into a mold and heat loss through the mold walls results in solidification of the alloy begining at the walls and proceeding inward. Overall, the solidification has no single direction. With directional solidification heat is extracted from only a single end or area of the mold, while the rest of the mold is insulated or is heated, thus creating a unidirectional temperature gradient in the melt. The nucleation for the solidification of the melt is favored at the cooled area and, as the cooling continues, the solidification proceeds following the direction of the temperature gradient imposed by the cooled area. The result is the directional solidification of the casting.

The solidification of an Al 6.2 wt.% Ni eutectic results in the formation of an aluminum phase with about .05 wt% Ni in solid solution and an intermetallic phase of Al_3Ni, as seen by the phase diagram of Figure 1 . By controlled undirectional solidification, the morphology of the Al_3Ni phase may take on two forms, as found by Lemkey [5]. At slow solidification rates, the Al_3Ni forms in parallel alternating platelets, becoming more rodlike in shape as the solidification rate is increased. At solidification speeds of 2.6 cm/hr and faster the Al_3Ni is primarily in rod shape.

It was also found that the inter-rod spacing is dependent on the solidification rate of the eutectic [5]. Increasing

the solidification rate decreases the inter-rod spacing with an inverse square root dependence on the speed of solidification. Decreasing the rod spacing has also been found to decrease the rod diameter. Usual fiber diameters obtained in composites such as the one in the present study are in the order of .5 to 1 um.

Breinan [6] reports that the microstructure produced in his Al-Al_3Ni composites was not completely uniform, but rather contained some faults. The structure reported by Breinan was characterized by alternating layers of misaligned fibers, called a dual orientation microstructure. This dual orientation was found to diminish as the solidification speed was increased. However, Breinan also notes that at higher solidification speeds (above 13 cm/hr) a colony structure becomes prominant where the eutectic microstructure forms longitudinal cells surrounded by areas depleted in Al_3Ni whiskers.

For purposes of deformation studies a microstructure with the least faults possible and with little or no cellular structure is desired. The choice of studying composites grown at high speed may result in less dual orientation faults but will also result in a highly cellular structure. A slow solidification rate would have the opposite effect of possibly giving a single crystal but containing many faults. Chosen here for study were composites grown at 8 cm/hr as this appeared to be a good speed below which no

cells would form and dual orientation faults would not be too predominant.

STRENGTH

The strength of a composite in the axis of its fiber direction is given by the rule of mixtures as

$$\sigma = V_1 \sigma_1 + (1 - V_1) \sigma_2$$

where σ is the composite strength, σ_1 is the fracture stress of the fibers, σ_2 is the stress in the matrix at the fiber fracture strain, and V_1 is the volume fraction of fibers in the composite. This equation assumes that the strains in the matrix and fibers are identical, that the fibers are infinitely long and that the composite fails when the fibers fail. Individual whisker strengths for Al_3Ni have been found to be in excess of 2070 MPa [7] and taking the matrix strength to be 34.50 MPa at the fracture strain of the fibers (approx. 2%) gives as a conservative composite strength

$$\sigma = (.1) 2070 + (.9) 34.5 = 238 \text{ MPa}$$

This strengthening is a result of the matrix transfering the majority of its load to the fibers by shear at the fiber matrix interface. At room temperature the matrix carries about 10-13 % of the load and the fibers carry the rest.

The assumption made in the rule of mixtures that the fibers are infinitely long in the matrix is not in reality true. We can however treat them as infinite fibers if they are at least 10 times greater than the critical fiber length, or the shortest fiber length in which a stress can be built up sufficient to fracture the fiber. This critical length is defined as

$$l = \sigma_1 r/\tau$$

where σ_1 is the fracture strength of the fiber, r is the radius of the fibers and τ is the shear stress of the matrix. If we consider the composite under study here, where σ_1 = 2070 MPa, r = .5 um and τ = 13.8 MPa, the critical fiber length is

$$l = 2070 \times .5\times10^{-6} / 13.8 = 75 \text{ um}$$

In the present study, to be considered infinitely long the fibers must be about 750 um long or have an aspect (length:diameter) ratio greater than 750. Hertzberg, et al.[7], obtained aspect ratios greater than 10 000 in composites solidified under conditions similar to the present study. Therefore, the infinite length argument is justified and the rule of mixtures should hold.

CREEP MECHANISMS

At temperatures above one-half the absolute melting temperature, metals will undergo continual plastic deformation when subjected to a constant stress. This occurs as a result of several mechanisms involving thermally activated migration and climb of dislocations, grain boundary shearing and diffusion of vacancies. These mechanisms fall into two major categories: those that refer to the stress directed diffusion of vacancies and those that refer to dynamic recovery by climb.

Diffusional Creep

The application of an internal stress can direct the diffusion of defects through a crystal or around the grain boundaries in a polycrystal. The vacancies flow through or around the grains of a metal, causing the grains to elongate in the direction of the applied stress. Here boundaries and sub-boundaries act as sources and sinks for the vacancies with the rate controlling process being either the diffusion of vacancies (diffusion controlled) or the rate of emission or absorbtion of the vacancies (source controlled). In diffusion controlled creep the strain rate will vary linearly with stress [8] and the activation energy for creep will be that of grain boundary or lattice diffusion, depending on whether the vacancy transport is along the boundaries or through the lattice. Diffusional creep is structure dependent; a metal with a large grain size will favor diffusion

through its lattice and a metal with a small grain or subgrain size will favor diffusion along its boundaries.

In source controlled diffusion, it is the rate of the interface reactions in the grain boundaries producing vacancies which controls the creep process. Burton [9] has developed an equation for source controlled dislocation creep predicting that the strain rate is proportional to the square of the applied stress and the activation energy for creep is either that of grain boundary or lattice diffusion. In materials of small grain size it is the source controlled process that is most likely to be rate controlling [10].

Dislocation Creep

In diffusional creep the sources and sinks for vacancies are grain boundaries, but in dislocation creep dislocations can also act as sources and sinks for vacancies. Thus a form of dislocation creep would be the diffusion of vacancies from dislocation half planes resulting in the climb of dislocations. The resulting deformation is diffusion controlled but the strain rate is now a nonlinear function of stress. This is because the creep rate is not only dependent on the crystal structure but is also dependent on the dislocation density which, is a function of stress.

In dislocation creep there are two competing factors occurring in the crystal; the motion and climb of dislocations, resulting in the recovery or coarsening of the dislo-

cation cell size, and the straining of the crystal, causing the material to harden or to refine its cell size. In steady state creep there must be a balance between the work hardening and recovery processes, giving rise to an equation for the steady state creep of a material. Several theories for dislocation creep exist [11,12,13] presenting different models for recovery and work hardening in the creeping metal, but they all predict an exponential power stress dependence of the creep rate with the power being in the range of 3-5.

DEFORMATION MAPS

Of the many mechanisms by which a material may deform at high temperature, there is usually one dominant mechanism in operation for a given field of stress and temperature. In a paper by Ashby[14], it was shown that the various fields in which a particular mechanism is dominant could be displayed pictorially on a single diagram to give what is known as a deformation map. With these maps it is possible to consolidate many theoretical and experimental results over a wide range of stresses and temperatures, thereby making these maps useful tools for the prediction of mechanical behavior in design work.

In the case of aluminum there appear to be five different deformation mechanisms by which creep can occur [15]. These are listed in Table 1. Three of these mechanisms arise from

diffusional creep, with the flow of vacancies taking place either through the lattice, in which case either Harper-Dorn or Nabarro-Herring creep is predominant, or along the grain boundaries, which gives rise to Coble creep. At higher temperatures a stress power law creep is observed and is generally attributed to some form of dislocation creep. If the vacancies involved in climb diffuse along the dislocation cores at low temperatures, low temperature climb occurs. When the vacancies diffuse through the crystalline lattice at high temperatures, high temperature climb occurs. These five mechanisms operate independently and each have a constitutive equation for the creep strain rate.

A deformation map for aluminum [16] is shown in Figure 2 where the axes represent the normalized stress, σ/G, versus the reciprocal of the homologous temperature, Tm/T. The boundaries separating the mechanism fields are found by equating the constitutive equations of neighboring mechanisms. The field boundaries are given by straight lines with the slope given by

$$\text{slope} = (\Delta Q/2.3RTm)/\Delta n$$

where ΔQ and Δn are the differences in the activation energies and the stress exponents for the two mechanisms on either side of the boundary.

Lines of constant strain rate may be inserted on the map, as in Figure 2, to display approximately the steady state

creep rate. This is done by solving the constitutive equation for a selected strain rate in its proper field and then drawing a straight line through this point within the field, with a slope given by

$$\text{slope} = Q/n\ 2.3RTm$$

where the value of Q and n are of the appropriate mechanism. It can be seen that strain rate contours an order of magnitude apart are equally spaced within any field, the spacing being 1/n when measured parallel to the normalized stress axis. Also the slope of the line will change when entering another field which has either a different activation energy or a different stress exponent.

EXPERIMENTAL PROCEDURES

ALLOYING AND SOLIDIFICATION

The Al(rich)-Ni eutectic was prepared by melting approximately 350 grams of high purity aluminum (99.999%) in a graphite crucible and adding the appropriate amount of nickel (99.99%) to give the 6.2 wt.% Ni eutectic. Argon was bubbled through the melt prior to casting to remove oxygen. The alloy was cast into 160 mm by 25 mm diameter rod using graphite molds.

Directional solidification was achieved by placing the alloy and graphite mold in a travelling resistance furnace, as shown in Figure 3, remelting the alloy while under an argon atmosphere and raising the furnace from the melt at a constant rate of 8 cm/hr.

SPECIMEN PREPARATION

The directionally solidified ingots were cut along their length into blanks with an abrasive saw and the blanks milled to approximately 2.4 mm thickness. Flat tensile specimens with gage lengths of 20mm and 38 mm parallel to the growth direction and 3.8 mm gage width were cut from the blanks on a numerically controlled milling machine. Usually two specimens could be made from each ingot, using only the

center part of the ingot. The specimens with the longer gage length of 38 mm were used for tests at slow strain rates to obtain a better sensitivity of strain measurement.

TENSILE TESTING

The tensile strength of the Al-Ni composite was determined on a standard 20 mm gage length creep specimen to compare the integrity of the composite with that of previous investigations. The testing was done on an Instron testing machine at a constant strain rate of 2.5 mm per min. at room temperature.

CREEP TESTING

Specimens were tested on Satec constant load creep machines equipped with resistance heated, 3 zone furnaces. Elongations were measured from points taken on the grips using a mechanical extensometer and an LVDT. Tests were run at 5 stress levels: 6.90, 17.3, 34.5, 43.8 and 69.0 MPa. The stress levels were accurate to within ± .34 MPa. The testing temperatures, ranging from 812 K to 375 K, were measured with chromel/alumel thermocouples loosely tied to the specimen gage length and were controlled to ± 2 K. The steady state creep rates for all the specimens were determined at approximately 2 % strain. For specimens tested at the lower strain rates, several steady state creep rates were obtained from a single specimen by increasing the temperature in suc-

cessive steps while keeping the stress constant. The error in the measured creep rate for the two types of tests has been estimated to be 25% [17] and is considered sufficiently accurate for the present investigation.

FRICTION STRESS DETERMINATION

The friction stress was determined using the stress decrement method as described by Davies, et al.[18]. A creep test is run until steady state is attained. Then, a small fraction of the load is removed, as shown in Figure 4. An incubation period of zero creep follows the removal, the duration of which is recorded and the stress is again reduced when the creep recommences. Consecutive small stress reductions are made in this way and a plot of the cumulative incubation period versus the cumulative stress reduction is made, as shown in Figure 5. These graphs appear to reach a limiting value at the friction stress

$$\sigma_0 = \sigma - \Sigma \Delta\sigma$$

where $\Sigma \Delta\sigma$ is the total stress removed and σ is the initial applied stress. These tests were performed at three temperatures in the same temperature range as the creep tests.

RESULTS AND DISCUSSION

MACROSTRUCTURE

An etched longitudinal section of a unidirectionally solidified ingot is shown in Figure 6, where the direction of solidification is from left to right. A columnar structure was observed to extend throughout the whole length of the ingot, giving rise to the apparent "wood grain" appearance. For the most part there is only a slight deviation of the columnar grains from the longitudinal axis of the ingot. Figure 7 shows a transverse section of an ingot, which shows the cross section of the columnar grains. These grains consist of packets or cells of eutectic microstructure surrounded by areas depleted in whiskers, with the average diameter of the cells being approximately 1 mm. Lemkey [5] reports no cell formation at solidification speeds below 13 cm/hour, but the many nucleation sites inside the graphite mold, the lower purity alloy used here and the temperature gradient in the solidification process may have contributed to the breakdown of the planar solid/liquid interface needed to produce a single crystal ingot. However, given the good alignment and the continuous nature of the columnar grains, the integrity of the composite is expected to be maintained.

MICROSTRUCTURE

A longitudinal section of the composite microstructure is shown in Figure 8, where the growth direction is from left to right. The micrograph shows the aligned orientation of the whiskers in the growth direction, but does not actually show their true length since the whiskers are not exactly parallel to the polishing plane and only a section of their length is visible. It is estimated that the average fiber length is greater than 1000 um, giving aspect ratios in excess of 1000.

Overall, the structure of the eutectic was uniform but did contain some faults, predominantly the fiber misorientation discussed earlier. This duel orientation microstructure occurs over a large range of solidification rates and would be difficult to avoid in the solidification of the composites produced here.

TENSILE PROPERTIES

Figure 9 shows the strengthening effect of whisker alignment in the composite. As is seen, unidirectional solidification increases the strength of the eutectic almost three-fold over that in the as-cast condition. The composite is found to obey the rule of mixtures, displaying a kinked flow curve and a fracture strain of about 2% since the failure of the composite occurs with the fracture of the brittle fibers. The experimental ultimate strength of 221 MPa compares well

with the strength predicted by the rule of mixtures and with values in the range 240-300 MPa obtained in previous investigations [5,7]. Therefore, it can be assumed that good fiber strengthening has been achieved in the composites produced here.

CREEP DEFORMATION BEHAVIOR

The creep behavior of the directionally solidified eutectic exhibited the three stages of the conventional creep curve as shown in Figure 10. From Table 2 the elongation of most of the specimens tested to fracture was in the order of 10-15%, but some specimens broke at strains as high as 30%. From a visual examination of the fractured specimens, it was noticed that the specimens which broke at elongations above 15% demonstrated some necking and were failing and creeping faster than would be expected from the data of the other specimens. The necking and premature failure of the specimens tested can be explained by the faults in the microstructure described earlier. According to Breinan, et al.[6], the fiber misalignment can effect the fracture behavior of the composite if the fibers are oriented in such a way (as in the dual phase microstructure) as to allow the matrix to deform at low stress. Since the fiber misalignment seems to occur by chance and by varying amounts in the material, this would give rise to the scatter observed in the creep and fracture behavior of the composite.

APPARENT ACTIVATION ENERGY

The temperature dependence of the steady state creep rate of the composite is shown in Figure 11, assuming that the creep rate can be expressed in the form

$$\dot{\epsilon} kT = A\, D_0 Gb\, (\sigma/G)^n \exp(-Q/RT)$$

where T is the absolute temperature, G is the shear modulus, A is a constant, D_0 is the frequency factor, b is the Burger's vector, k is Boltzman's constant, σ is the applied stress, n is the stress power constant and Q is the creep activation energy. In all calculations, the value of the temperature dependent shear modulus, G, was taken as that of aluminum [16], as it is considered to be representative of the temperature dependence of the composite's shear modulus.

As can be observed in Figure 11, there appears to be at least two distinct activation energy levels for the creep of the composite. For each stress level there appears to be a temperature above which the activation energy is high, in the order of 159-231 kJ/mole, and below which the activation energy is low, in the order of 42-74 kJ/mole. The activation energy in the upper temperature range is somewhat higher than the activation energy for self diffusion of aluminum, reported to be between 126-143 kJ/mole [19,20]. However the activation energy in the lower temperature range is comparable to the activation energy for grain boundary diffusion estimated to be approximately 86 kJ/mole [16].

APPARENT STRESS EXPONENT

The value of the stress exponent, n, is usually found by plotting the strain rate versus the normalized stress at constant temperature. Figure 12 shows such a plot, where the data have been taken from Figure 11. The slopes vary from 1.8 to 12 depending on the state of stress and temperature of the creep test.

To obtain a clearer understanding of the stress behavior of the composite, the data in the high and the low activation energy fields are studied separately. The average value of the activation energy for a field is used to obtain a representative diffusion coefficient for each of the fields. Then, by plotting the strain rate divided by the diffusion coefficient of its respective field versus normalized stress, stress exponents of the various mechanisms are obtained as shown in Figures 13 and 14. From the figures it would appear four different creep behaviors exist, displaying different stress exponent values of 2.4, 4.9, 7.6 and 13.9.

DEFORMATION MAP

A deformation map for the composite was produced from the information of Figures 13 and 14 and is shown in Figure 15. The solid lines represent the field boundaries and the dashed lines are lines of constant strain rate, $\dot{\epsilon}T/G$. In Figure 15 the four distinct mechanisms or constitutive equa-

tions which exist to describe the creep of the composite are now apparent, each of which is dominant in its own stress and temperature field. However, the map is only a rough approximation of the creep behavior since it has been assumed here for simplicity that there are only two values of the activation energy for creep. For example, this assumption will mean that the boundary between fields I and III and fields II and IV will be temperature independent, hence they are horizontal lines. With this in mind, an attempt is now made to identify the four apparent mechanisms of creep of the composite.

In the low temperature-low stress field of region IV of the creep map the stress exponent is approximately 2.4 and the activation energy for creep is in the order of 70 kJ/mole. This is typical of a Coble creep mechanism which for pure aluminum is given by [15]

$$\dot{\epsilon} kT = 124\ Gb \exp(-Q/RT)\ (b/d)^3\ (\sigma/G)$$

where d is a lattice dimension usually taken as the grain size. If an interfiber spacing of 2 um is taken as a characteristic matrix dimension, d, creep rates predicted by this equation are in the range of those observed in the composite even if the matrix is considered to carry all of the applied load. The activation energy of approximately 70 kJ/mole observed here is in close agreement with the activation energy for grain boundary diffusion which controls Co-

ble creep. The stress exponent of 2.4 is higher than that of 1 for Coble creep, but this may be due to the contribution of another underlying mechanism not yet dominant, or variability in the data, since this region of testing is near the limit of detection for creep with the equipment used.

Looking at the stress exponent in region II of Figure 15, n=7.6 and the activation energy is approximately 70 kJ/mole. This value of stress exponent is considered high for creep controlled by dislocation climb. However Weertman [21] proposes a model for high temperature creep where, in an intermediate temperature range, the strain rate follows a 7th power dependence on stress and the activation energy for creep is that of pipe diffusion. The model proposes that above this intermediate temperature the stress dependence follows a natural fifth power and the activation energy for creep is that of self diffusion. In region III of the map, the stress exponent is approximately 5 but the activation energy for creep is somewhat higher than that for self diffusion. At higher stresses, however, the stress dependence rises to approximately 13.9 with an activation energy higher than that for self diffusion of aluminum. Creep of the intermetallic phase of Al_3Ni is thought to have such a high stress dependence [22] but its activation energy for diffusion is much higher than the one seen here (a value of 690 kJ/mole is reported [23]). Thus Weertman's model can pre-

dict the composite behavior in region II but does not correlate with the activation energy in region III and is unable to explain the high stress and temperature dependencies of region I. Also, the creep behavior of the composite cannot be directly attributed to creep of the Al_3Ni phase.

STRESS AND TEMPERATURE DEPENDENCE ASSUMING A THRESHOLD STRESS

The high value of the stress exponent in region I would suggest that another approach be taken in characterizing the deformation behavior of the composite. By assuming the presence of a threshold stress, σ_0, [18,24] which opposes the action of the applied stress, the creep rate equation would now become

$$\dot{\epsilon} kT = A_0 D_0 Gb[(\sigma - \sigma_0)/G]^{n_0} \exp(-Q^*/RT)$$

where Q* is the activation energy for the creep process and n_0 is the new stress exponent. The presence of σ_0 will result in the stress exponent, n_0, being lower than the apparent stress exponent, n, and the temperature dependence of σ_0 will cause Q* to be lower than the apparent activation energy, Q. Usually n_0 will be in the range of 3-5 which is that normally accepted for creep controlled by dislocation climb and the value of the activation energy, Q* , is generally close to the activation energy for lattice self diffusion. This was the approach taken by Himbeault and Cahoon [31] who found that n_0 = 3.5 and Q* = 104 kJ/mole for creep of

Al(rich)-Ni eutectic in the temperature range of 450-630 K and stress range 34.5-69.0 MPa.

The temperature dependence of the threshold stress, σ_0, found from stress change experiments is shown in Figure 16. The value of σ_0 is assumed to be independent of the applied stress [25] and tends to zero at the melting point [26], therefore the eutectic melting point (913K) has been included in the data. Generally, σ_0 values determined by the stress decrement method are higher than their actual values [25] and indeed better correlations were obtained in the calculations that follow if σ_0 values represented by the dashed line in Figure 16 were used. As is seen these values are only slightly lower than the experimental values.

If $\ln \dot{\epsilon}T/G$ is plotted versus $\ln(\sigma-\sigma_0)/G$ at constant temperature the slope will give the value of the stress exponent, n_0 . Such a plot is shown in Figure 17 where the data have been taken from Figure 11. There appear to be two distinct regions on this plot where above 480K the value of n_0 is approximately 4.8± .2 and below 480K where n_0 is approximately 2.1± .1 . This would indicate that two possible mechanisms are operating. Therefore, further analysis of these two regions is undertaken treating each separately.

To obtain the activation energy for creep in the region where n_0 = 4.8, a graph, as shown in Figure 18, is plotted. The value of Q* which is determined from the slope of the

line in Figure 18 was found to be 116 kJ/mole. This value of the creep activation energy is a little lower than that for the self diffusion of aluminum (143-126 kJ/mole) and higher than that of the estimated value of grain boundary or core diffusion (86 kJ/mole). However, this activation energy is likely representative of the aluminum phase, since the activation energy for diffusion in the Al_3Ni fibers is high (690 kJ/mole). The value of n_0 =4.8 is in the range of 3-5 which is normally accepted for creep where dislocation climb is the rate controlling process and is close to the value of the stress exponent of 4.4 for the dislocation creep of aluminum [16]. This would lead to the conclusion that in this region of stress, assuming the existence of a threshold stress, climb in the aluminum phase is rate controlling where the stress exponent is 4.8 and the activation energy for creep is close to that of self diffusion in aluminum.

Figure 19 shows the plot used to obtain an activation energy for creep of 51.6 kJ/mole for the region where the stress exponent is 2.1. Gittus [27] proposes a model for creep controlled by dislocation climb at interphase boundaries of two phase materials where the value of the threshold stress compensated stress exponent would be 2 and the activation energy for creep would be that for interphase boundary diffusion. This model would certainly be in agreement with the creep behavior observed in the composite in this region if the activation energy for interphase boundary

diffusion were this low. Unfortunately, little information is available on the actual value of this parameter. Gittus does point out that the activation energy for self diffusion in interphase boundaries can be high, nearer to the value for volume diffusion than grain boundary diffusion. However a low value of the activation energy for interphase boundary diffusion should not be totally discounted.

Thus far, it has been shown that the creep of the Al(rich)-Ni composite can be described by three equations. These are

(1) $\dot{\epsilon} kT = 2.75 \times 10^{-13} D_0 Gb\{(\sigma-\sigma_0)/G\}^{2.1} \exp(-51\ 600/RT)$

(2) $\dot{\epsilon} kT = 258\ D_0 Gb\{(\sigma-\sigma_0)/G\}^{4.8} \exp(-116\ 000/RT)$

(3) $\dot{\epsilon} kT = 4.57 \times 10^{-13}\ D_0 Gb\,(\sigma/G)^{2.4} \exp(-70\ 000/RT)$

The fields of stress and temperature where each of these equations are dominant is shown in the deformation map of Figure 20. The value of the threshold stress is also shown on this figure. Figures 21 and 22 show plots of the above equations and compares them with the creep data. A good correlation with the data is evident.

RATE CONTROLLING PHASE

It appears the matrix phase is rate controlling in the creep of the composite since the creep parameters of the composite match more closely those for creep of aluminum than those suggested for the creep of the fibers when a threshold stress is assumed. This would imply the deformation of the fibers does not contribute significantly to the overall deformation behavior of the composite. Yet, the fibers must be carrying a significant portion of the load since fractured fibers have been seen throughout the gage length of creep tested specimens, as seen in the scanning electron micrograph of Figure 23. However, it is important to note that with discontinuous fibers the load transfer occurring from the matrix to the fibers requires a shear stress at the matrix/fiber interface. At room temperature these stresses are more highly localized at the fiber ends than along the length of the fiber and the average tensile stress in the matrix is low. At higher temperatures, where stress relaxation in the matrix can occur, the load transfer to the fibers must now occur by shear between the fiber and the matrix, creating longer range stresses at the fiber ends than at lower temperatures. This will lead to an increase in the average tensile stress in the matrix and a reduction in the fiber stress. Obviously the rule of mixtures no longer applies at high temperatures. Therefore, a different approach should be taken to study the state of stress in the composite.

In a phenomenological analysis of creep in fiber reinforced composites by deSilva [28], the creep of a composite is governed by stress relaxation in the matrix and by creep of the fibers. At negligible fiber creep rates, it is predicted that the creep of the matrix controls the creep of the composite with most of the matrix flow occurring at the fiber ends. McLean [29] and Mileiko [30] present similar approaches for the creep of aligned composites but consider only rigid fibers. The increase in flow resistance of the composite comes from the argument that the shear strain in the composite is greatly amplified compared with the shear strain in an unsupported matrix. This increased shear requires a greater expenditure of energy. Therefore, the tensile creep resistance of the material is increased. In these models the creep parameters of the composite are determined by the flow properties of the matrix.

These models agree at least qualitatively with the creep behavior observed in the Al-Ni composites studied in this investigation. Strengthening comes from an amplified matrix flow required to load the fibers. Therefore, because most of the flow occurs in the matrix, the creep parameters of the composite are those of the matrix. When the threshold stress is taken into account, the creep parameters of the Al(rich)-Ni eutectic composite are representative of aluminum. Creep in the fibers is assumed to be negligible in these models, which is realistic since the temperatures for

creep of the eutectic are low compared to those for the higher melting point Al_3Ni intermetalic compound.

The threshold stress likely arises from a form of dispersion strengthening occurring in the matrix due to the presence of the Al_3Ni fibers. The fibers interact with the dislocation movement in the matrix, pinning the dislocations at the matrix/fiber interface as has been observed by Breinan, et al.[31], using electron microscopy. To move these dislocations requires a stress over and above a specific stress, which is the threshold stress, σ_0 . The subsequent movement of the dislocations then occurs under an effective stress given by $(\sigma-\sigma_0)$, where σ is the applied stress.

The threshold stress is normally defined as the stress below which creep will not occur [32]. However, in this investigation, creep does occur below the threshold stress. Thus, in this study, σ_0 may be interpreted as a stress level separating two different creep mechanisms. This is indicated in Figure 20, where σ_0 is very close to the boundary between regions.

CONCLUSIONS

1. The creep rate of directionally solidified Al(rich)-Ni eutectic can be described by four equations of the form

$$\dot{\epsilon} kT = A\, G D_0 b (\sigma/G)^n \exp(-Q/RT)$$

where values of Q range from 231 kJ/mole to 42 kJ/mole and values of n range from 1.8 to 12.

2. With the inclusion of an experimentally determined threshold stress, the creep rate can be expressed by three equations

$$\dot{\epsilon} kT = 2.75 \times 10^{-13} D_0 Gb\{(\sigma-\sigma_0)/G\}^{2.1} \exp(-51\ 600/RT)$$

$$\dot{\epsilon} kT = 258\ D_0 Gb\{(\sigma-\sigma_0)/G\}^{4.8} \exp(-116\ 000/RT)$$

$$\dot{\epsilon} kT = 4.75 \times 10^{-13} D_0 Gb\,(\sigma/G)^{2.4} \exp(-70\ 000/RT)$$

3. By including the threshold stress, the stress exponents are in the range of 2-5, which is that accepted for creep controlled by dislocation climb. The activation energies for creep appear to be representative of either volume or grain boundary diffusion in aluminum and below that for diffusion in Al_3Ni .

4. Creep of the Al-Ni eutectic is believed to be controlled by creep of the Al matrix since the activation energies for

creep of 70, 116 and 51.6 kJ/mole could correspond to that of grain boundary or core diffusion, self diffusion and interphase boundary diffusion respectively.

5. Creep in the Al_3Ni fibers is thought to be negligible and the creep of the composite occurs by matrix flow at the fiber ends in the composite.

REFERENCES

1. N.S. Stoloff, Conf. on InSitu Composites, 3rd, Boston, Mass, Nov.29-Dec.1 (1978)

2. E.M. Breinan, E.R.Thompson and W.K. Tice, Met. Trans., 3, 211-219 (1972)

3. Y.G. Kim and N.S. Stoloff, Met. Trans., 5, 809-815 (1974)

4. M. McLean,'Directionally Solidified Materials for High Temperature Service', p.180, Metals Society, London (1983)

5. F.D. Lemkey, R.W. Hertzburg and J.A. Ford, Trans. Met. Soc. AIME, 233, 334-341 (1965)

6. E.M. Breinan, E.R. Thompson, G.P. McCarthy and W.J. Herman, Met. Trans., 3, 221-234 (1972)

7. R.W. Hertzburg, F.D. Lemkey and J.A. Ford, Trans. Met. Soc. AIME, 233, 342-354 (1965)

8. J.R. Spingarn and W.D. Nix, Acta Met., 27, 171-177 (1979)

9. B. Burton, Mat. Sci. Eng., 10, 9-14 (1972)

10. J. Gittus,'Creep, Viscoelasticity and Creep Fracture in Solids', p.26, Appl. Science Pub., London (1975)

11. J. Gittus, Acta Met, 22, 798-791 (1974)

12. J. Gittus,'Creep, Viscoelasticity and Creep Fracture in Solids', p.42-46, Appl. Science Pub., London (1975)

13. Z. Horita and T.G. Langdon, Proc. Second Int. Conf on Creep and Fracture of Engineering Materials and Structures (edited by B. Wilshire and D.R.J. Owen) 75-87, Pineridge Press, Swansea, Wales (1984)

14. M.F. Ashby, Acta Met., 20, 887-897 (1972)

15. T.G Langdon and F.A. Mohomed, Mat. Sci. Eng., 32, 103-112 (1978)

16. T.G. Langdon, Met. Forum, 1, 59-70 (1978)

17. E.C. Norman and S.A. Duran, Acta Met., 18, 723-731 (1970)

18. P.W.Davies, G. Nelms, K.R. Williams and B. Wilshire, Met. Sci. J., 7, 87-92 (1973)

19. T.E. Volin and R.W. Balluffi, Phys. Stat. Sol., 25, 163-173 (1968)

20. T.S. Lundy and J.F. Murdock, Heat Appl. Phys., 33, 1671-1673 (1962)

21. J. Weertman, Proc. Second Int. Conf. on Creep and Fracture of Engineering Materials and Structures (edited by B. Wilshire and D.R.J. Owen), 1-13 (1984)

22. M. Dorik and A.S. Yue, Met. Trans., 7, 1465-1468 (1976)

23. I.I. Komilov, A.Y. Shinayev and Y.N. Pyloyev, Izv. Akad. Nauk. SSSR, Russian Met. and Mining, 5, 67 (1973)

24. K.R. Williams and B. Wilshire, Met. Sci. J., 7 176-179 (1973)

25. M. McLean,' Directionally Solidified Materials for High Temperature Service', 184, Metals Society, London (1983)

26. B.A. Movchan and L.M. Nerodenko, Fizika Metall., 43, 338-397 (1977)

27. J.H. Gittus, Trans. ASME J. Eng. Mater. Technol., 99, 244 (1977)

28. A.R.T. DeSilva, J. Mech. Phys. Solids, 16, 169-186 (1968)

29. D. McLean, J. Mat. Sci., 7, 98-104 (1972)

30. S.T. Mileiko, J. Mat. Sci., 5, 254-261 (1970)

31. D. Himbeault and J.R. Cahoon, Can. Met. Quart. (in press)

32. W.J. Clegg and J.W. Martin, Met. Sci. J., 16, 65-72 (1982)

33. Metals Handbook, 8th edition, American Society for Metals, pp. 1164 (1948)

TABLE 1

Constitutive equations for creep of pure aluminum

Mechanism	Constitutive equation for $\dot{\epsilon}(s^{-1})$
Nabarro- Herring:	$\dot{\epsilon} = A_{NH} D_{o(l)} \exp(-Q_l/RT) \frac{Gb}{kT} \left(\frac{b}{d}\right)^2 \left(\frac{\sigma}{G}\right)$
Coble:	$\dot{\epsilon} = A_{Co} D_{o(gb)} \exp(-Q_{gb}/RT) \frac{Gb}{kT} \left(\frac{b}{d}\right)^3 \left(\frac{\sigma}{G}\right)$
Harper -Dorn:	$\dot{\epsilon} = A_{HD} D_{o(l)} \exp(-Q_l/RT) \frac{Gb}{kT} \left(\frac{\sigma}{G}\right)$
climb (L.T.):	$\dot{\epsilon} = 50 A_l D_{o(c)} \exp(-Q_c/RT) \frac{Gb}{kT} \left(\frac{\sigma}{G}\right)^{n+2}$
climb (H.T.):	$\dot{\epsilon} = A_l D_{o(l)} \exp(-Q_l/RT) \frac{Gb}{kT} \left(\frac{\sigma}{G}\right)^n$

A:	A_{NH}	$= 28$
	A_{Co}	$= 66.8$
	A_{HD}	$= 1.67 \times 10^{-11}$
	A_l	$= 2.5 \times 10^6$
D_o:	$D_{o(l)}$	$= 1.86$
	$D_{o(gb)}$	$= D_{o(l)}$
	$D_{o(c)}$	$= D_{o(gb)}$
Q:	Q_l	$= 143.4$ kJ mol^{-1}
	Q_{gb}	$= 0.6\, Q_l$
	Q_c	$= Q_{gb}$
G:	G	$= G_o - \Delta G T$
	G_o	$= 3.022 \times 10^4$ MPa
	ΔG	$= 16.0$ MPa K^{-1}
b:	b	$= 2.86 \times 10^{-8}$ cm
n:	n	$= 4.4$

TABLE 2

Summary of Creep Results

Stress psi	Temperature °K	Steady State Creep rate $sec^{-1} \times 10^{8}$	Time to Fracture hr.	Elongation at Fracture %
	812	20.4		
	788	6.17		
	765	1.85		
	750	2.78		
1000	731	.31		
	700	.11		
	679	.12		
	642	.062		
	614	.0019		
	690	9.26		
	675	2.65		
	651	2.06		
	648	1.80		
	620	.15		
2500	586	.05		
	583	.11		
	568	.080		
	531	.030		
	514	.040		
	633	146	4.1	12
	620	200	3.2	9
	608	52.0	18	15
	593	86.6	17	30
	575	13.0		
	573	6.2	134	10
5000	563	13.0	81	17
	556	2.53		
	544	.48		
	524	.18		
	496	.106		
	467	.090		
	593	1780	.7	15
	563	800	2	19
	543	29	22	14
	523	37.2	27	20
	498	6.7	118	12
	497	4.63		
7000	483	2.65		
	467	1.85		
	453	1.54		
	442	1.16		
	420	.25		
	408	.114		
	388	.050		
	543	4530	15	8
	523	249	4	14
	497	414	3	13
	488	31.6	38	14
	473	14.5	118	15
10000	456	7.6		
	445	8.23		
	431	2.10		
	393	.640		
	375	.450		

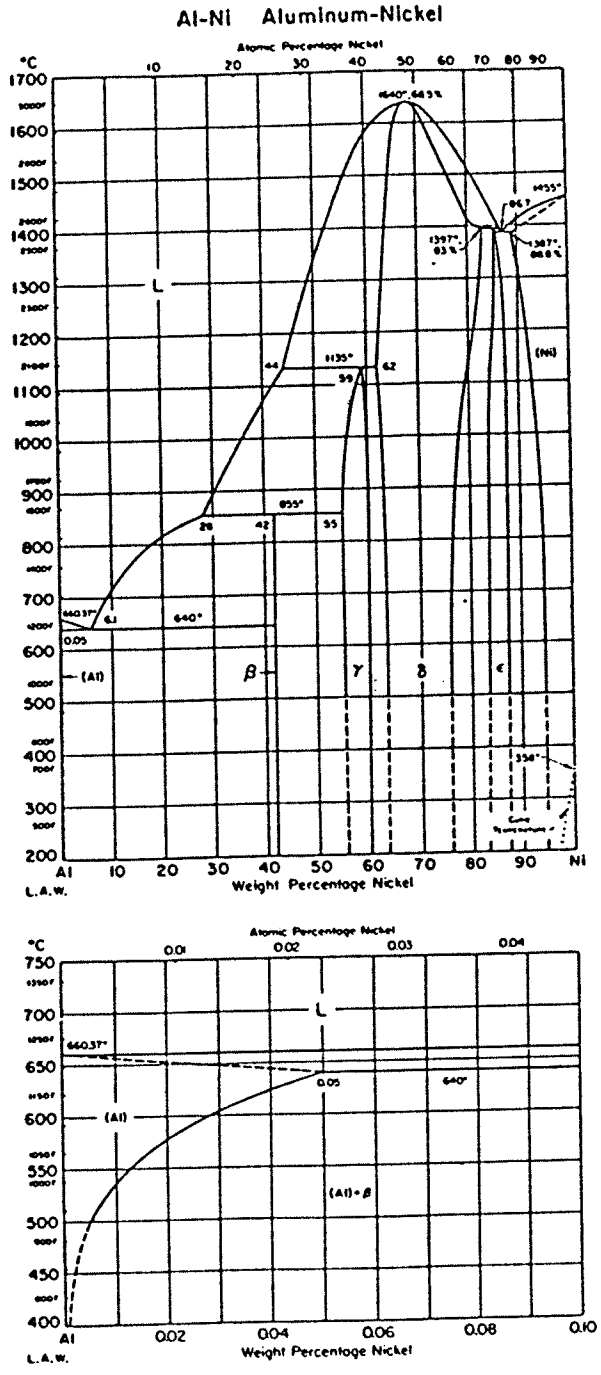

Figure 1: Phase diagram for Aluminum-Nickel [33].

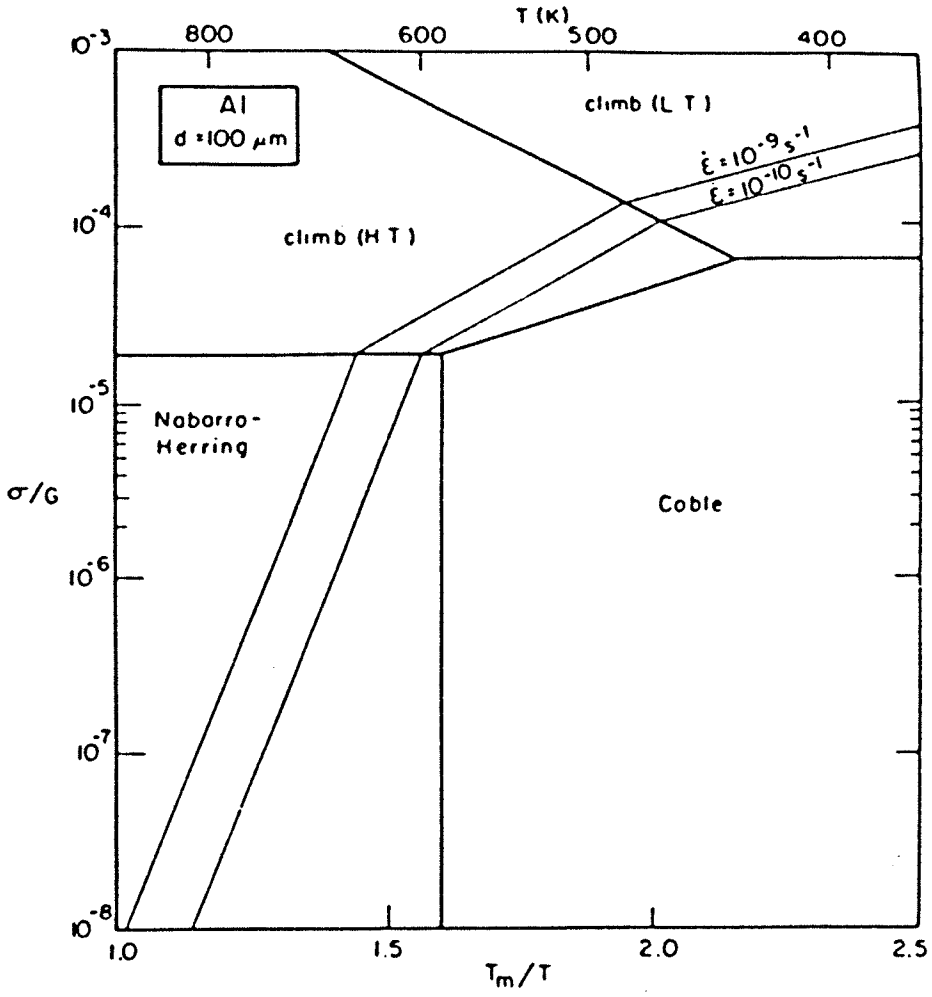

Figure 2: Deformation mechanism map for aluminum.

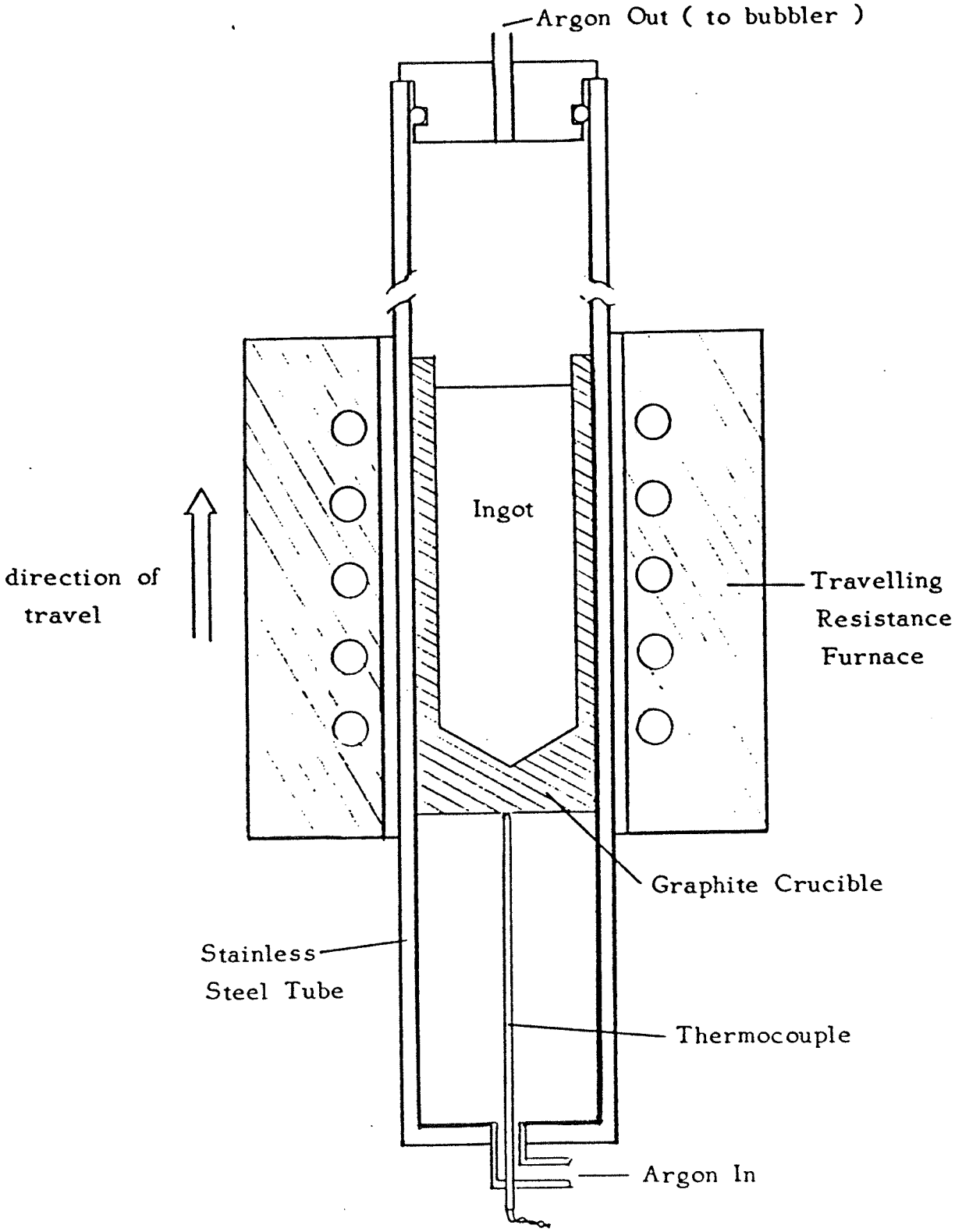

Figure 3: Cross section of solidification furnace.

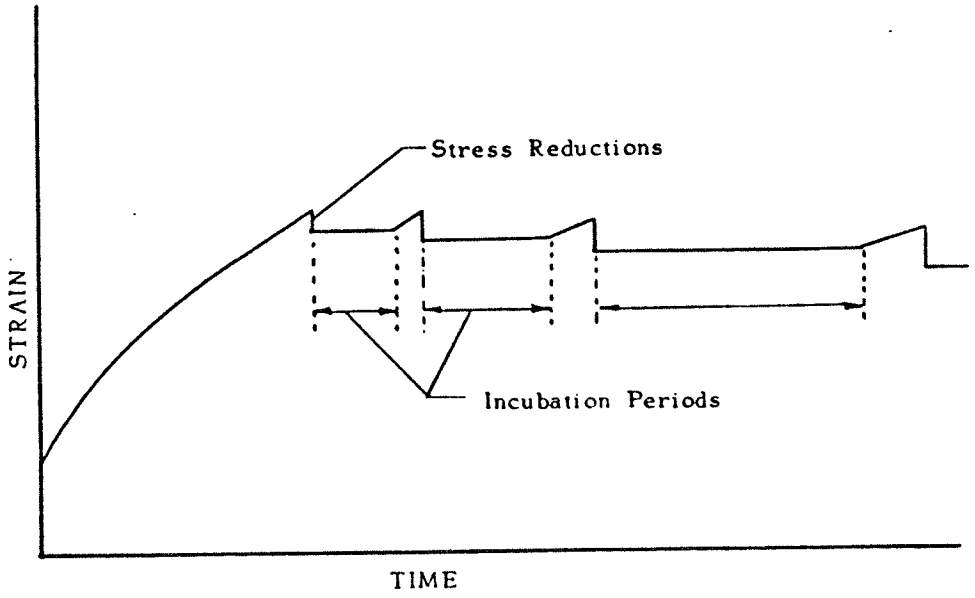

Figure 4: Representations of small stress reductions during a creep test.

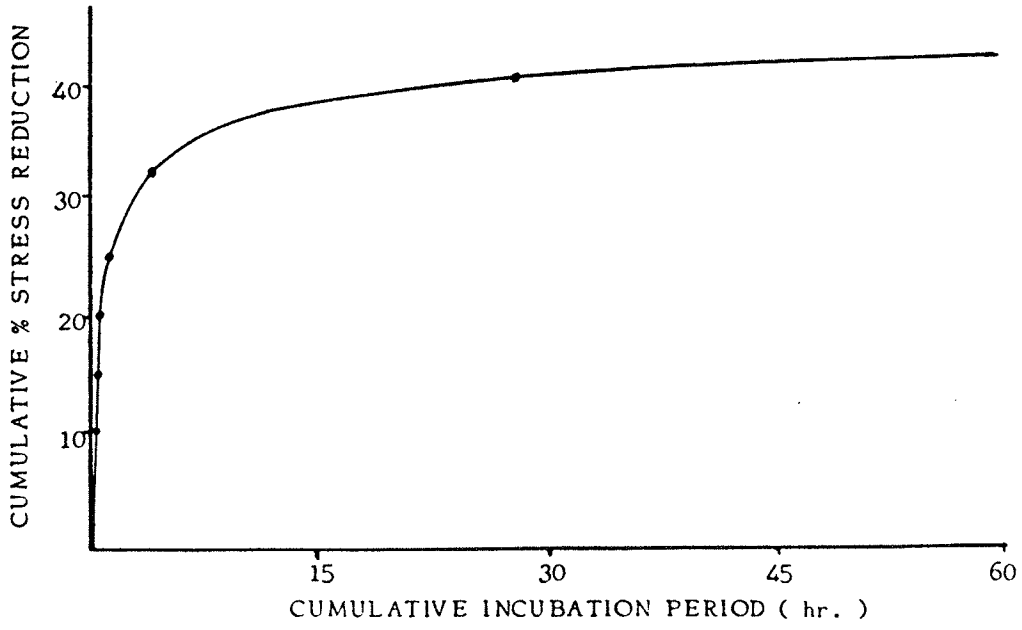

Figure 5: Example of a plot to determine the value of σ_0

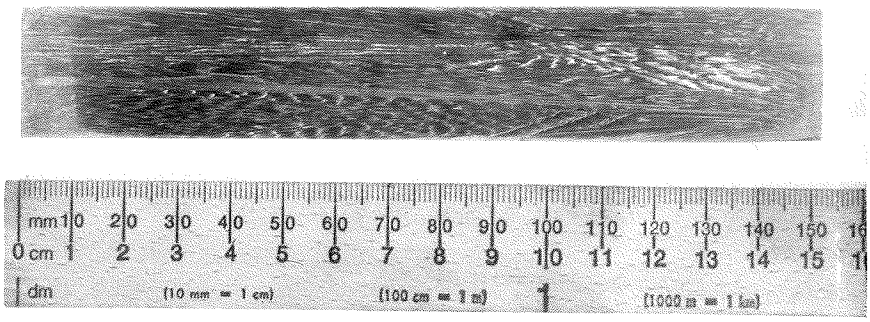

Figure 6: Longitudonal section of a directionally solidified ingot.

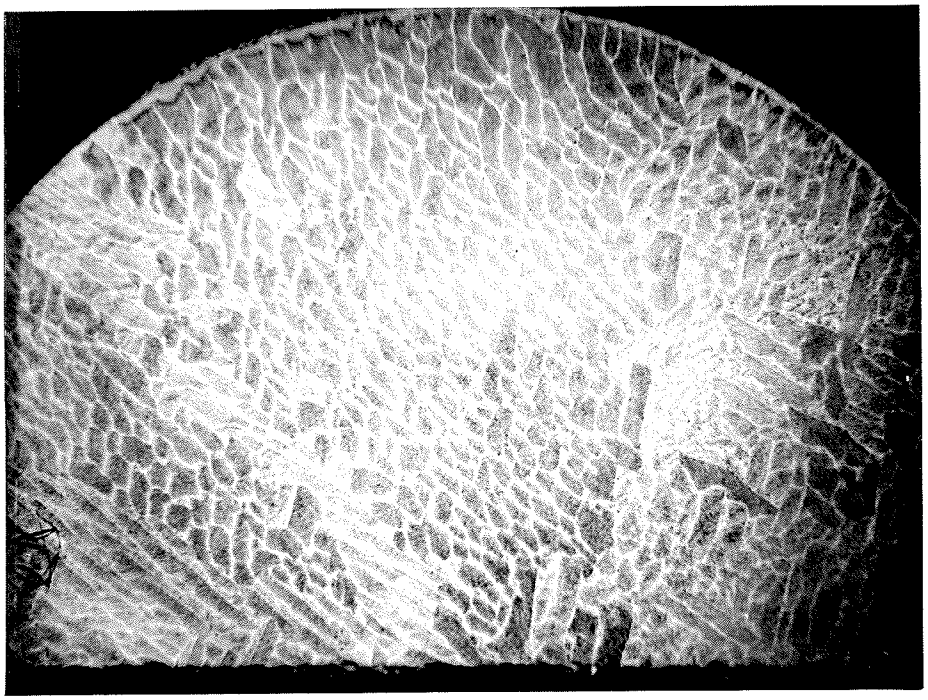

Figure 7: Cross-section of directionally solidified ingot.(5X)

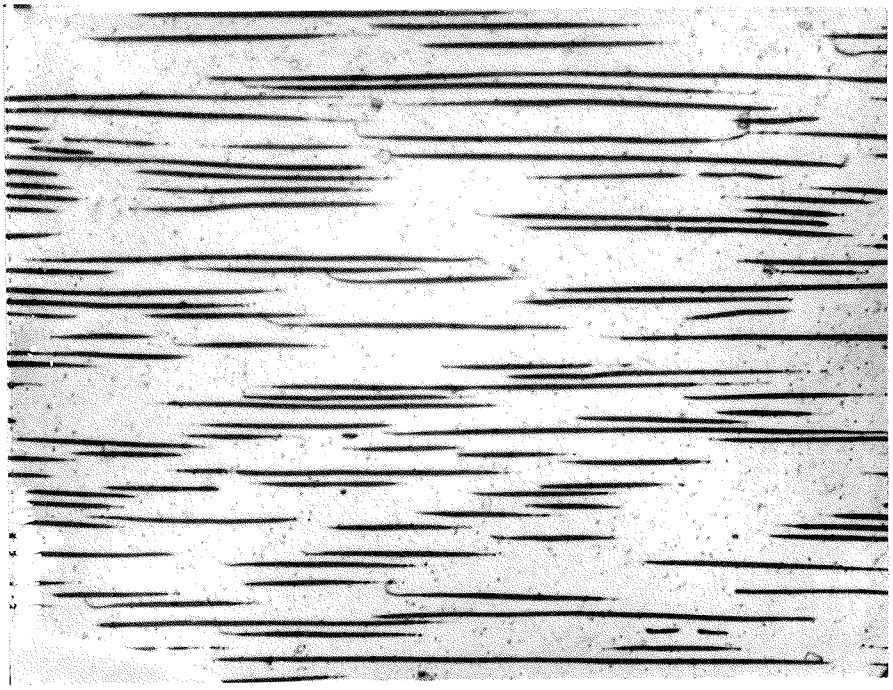

Figure 8: Micrograph of the composite microstructure.(1000X)

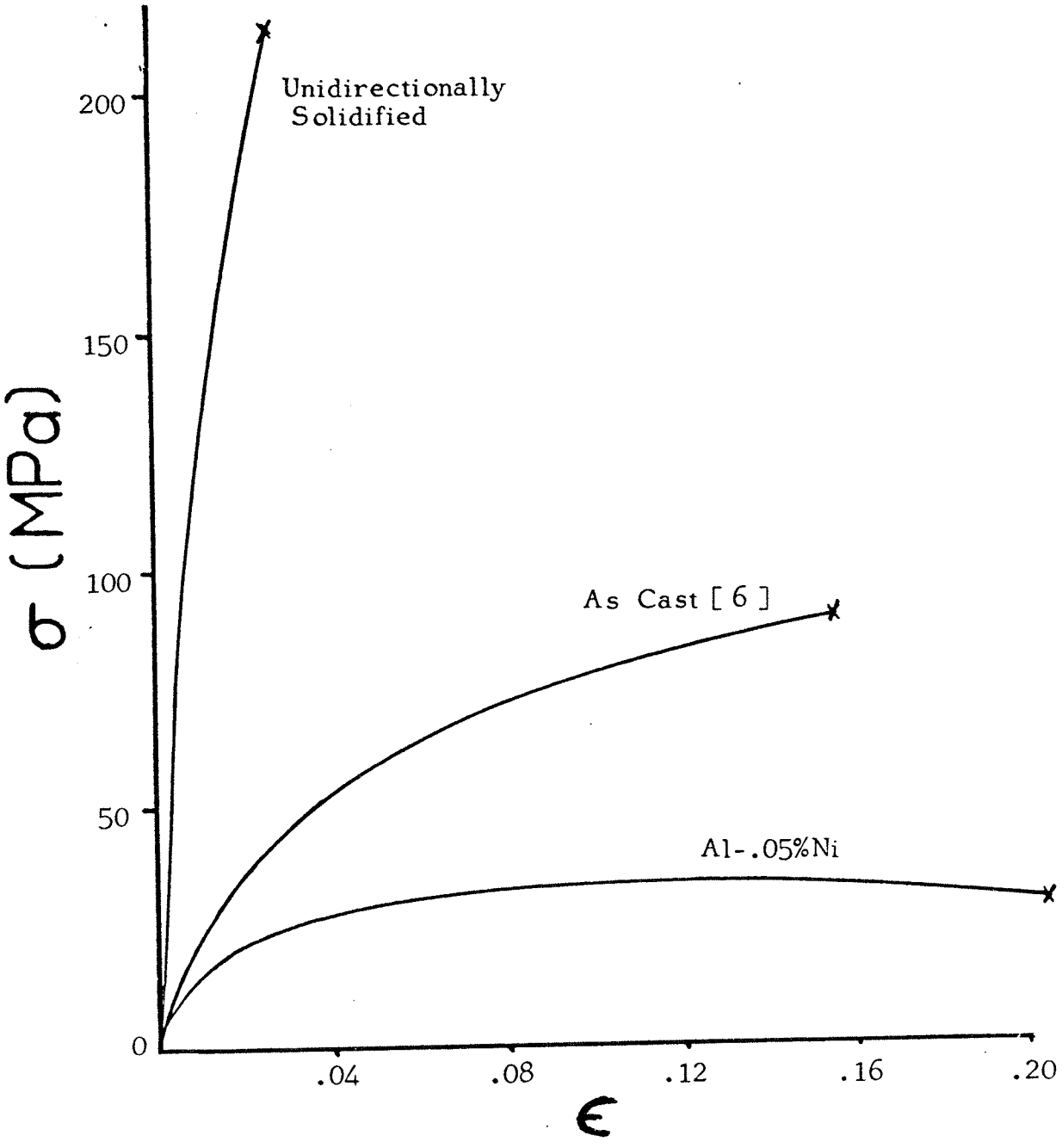

Figure 9: Flow curves for directionally solidified and as cast Al-Al_3Ni Al-.05%Ni alloy is included for comparison with matrix material.

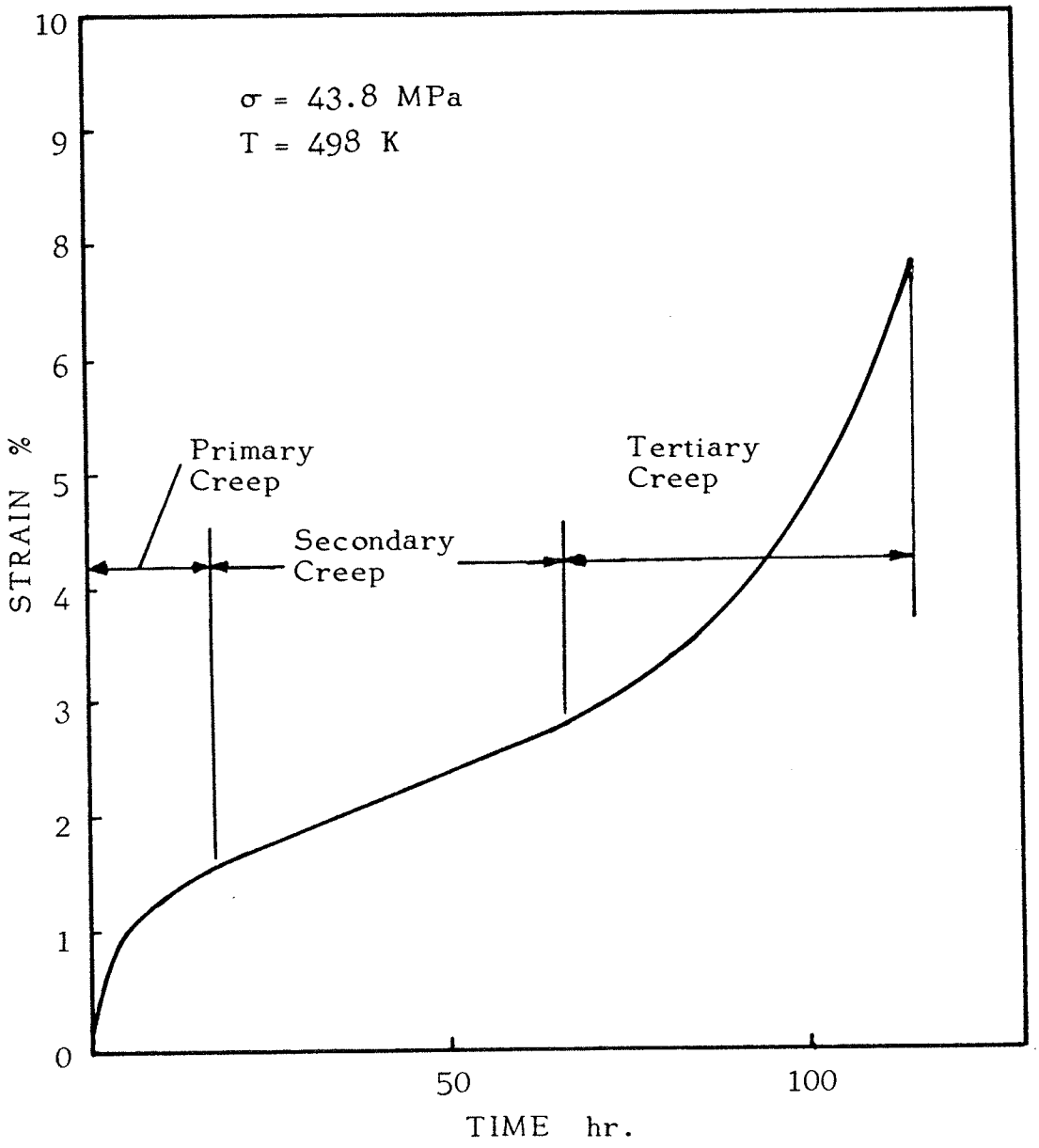

Figure 10: Example of a creep curve for Al(rich)-Ni composite.

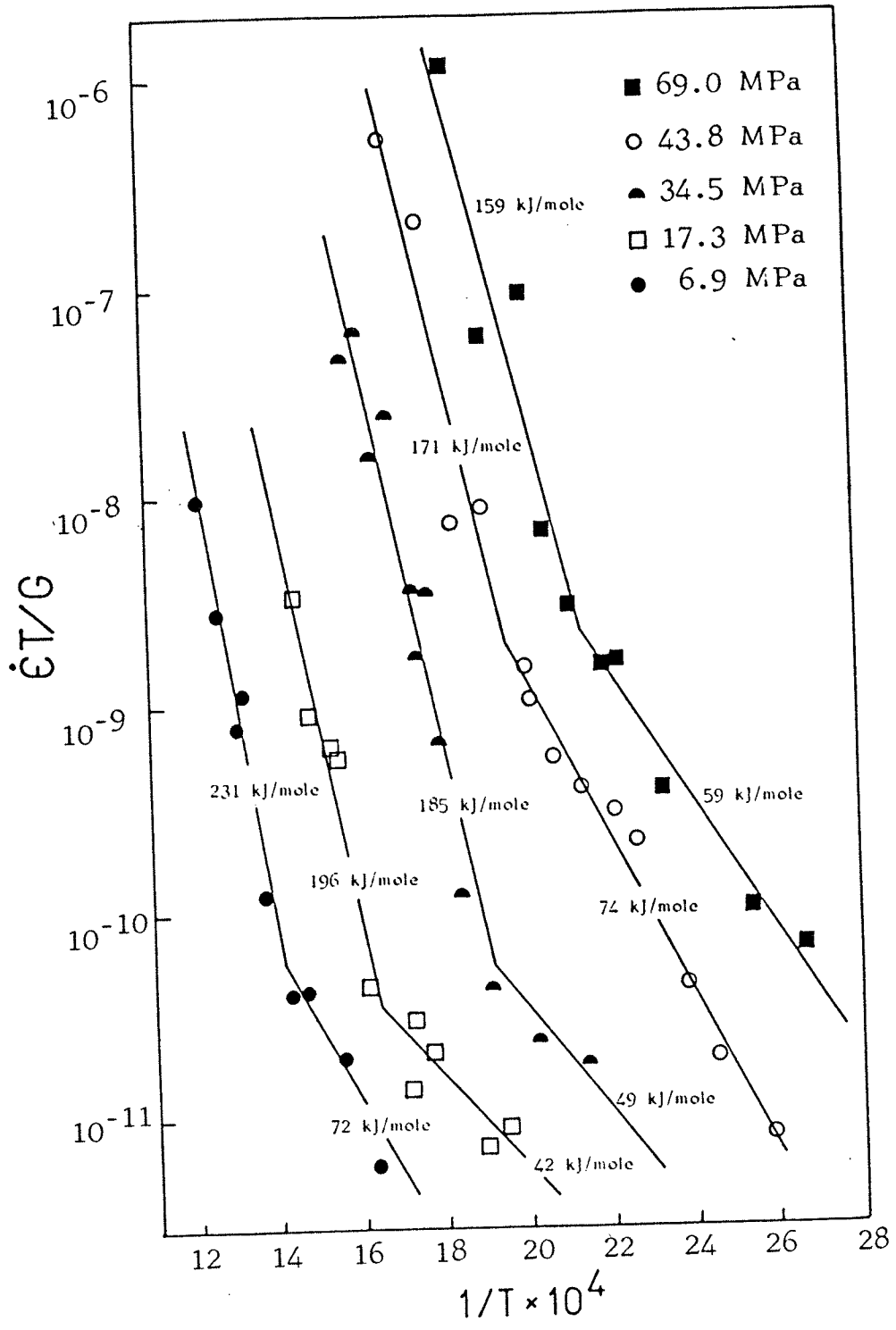

Figure 11: Creep rate of Al-Ni composite.

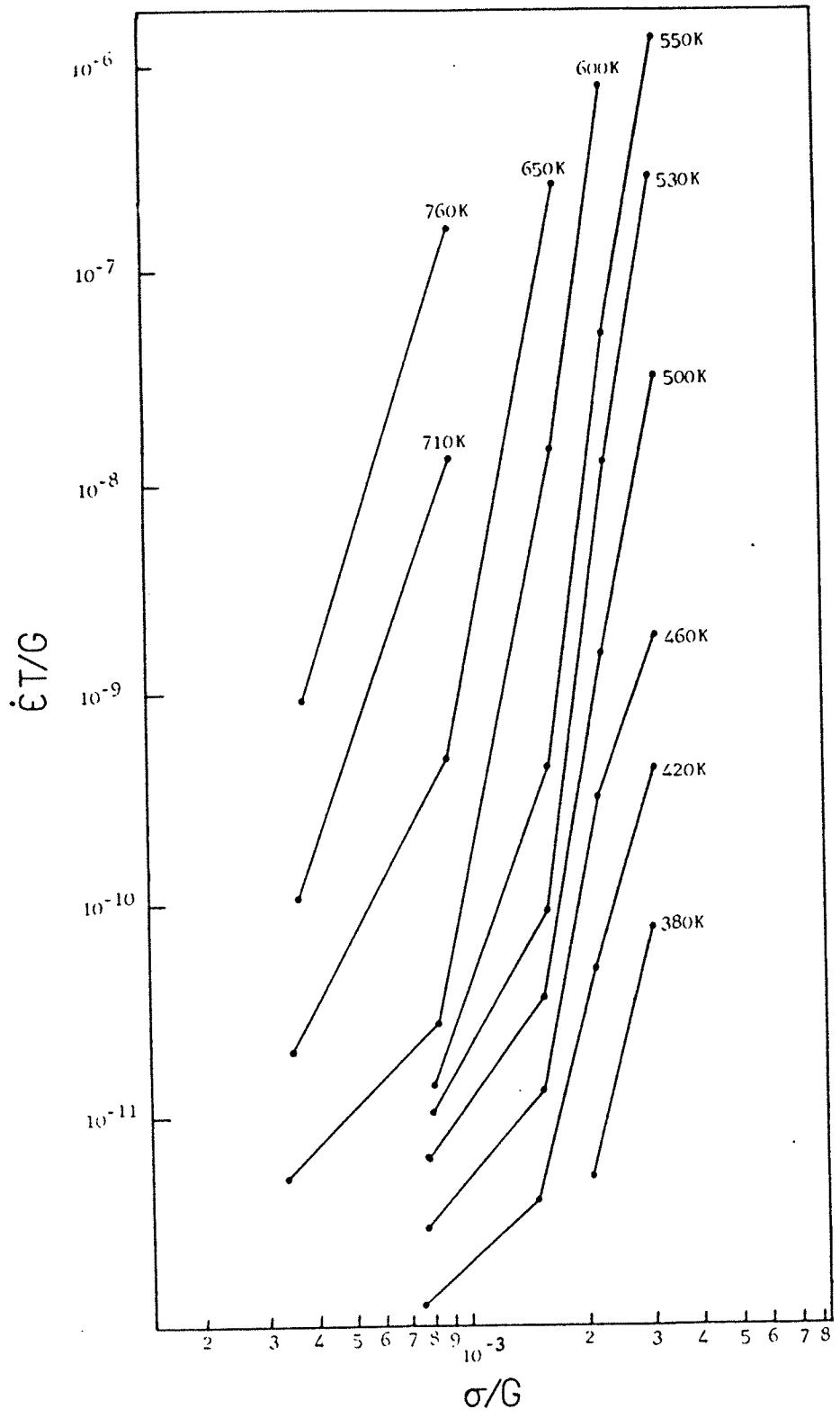

Figure 12: Determination of the stress exponent for creep of Al-Ni eutectic.

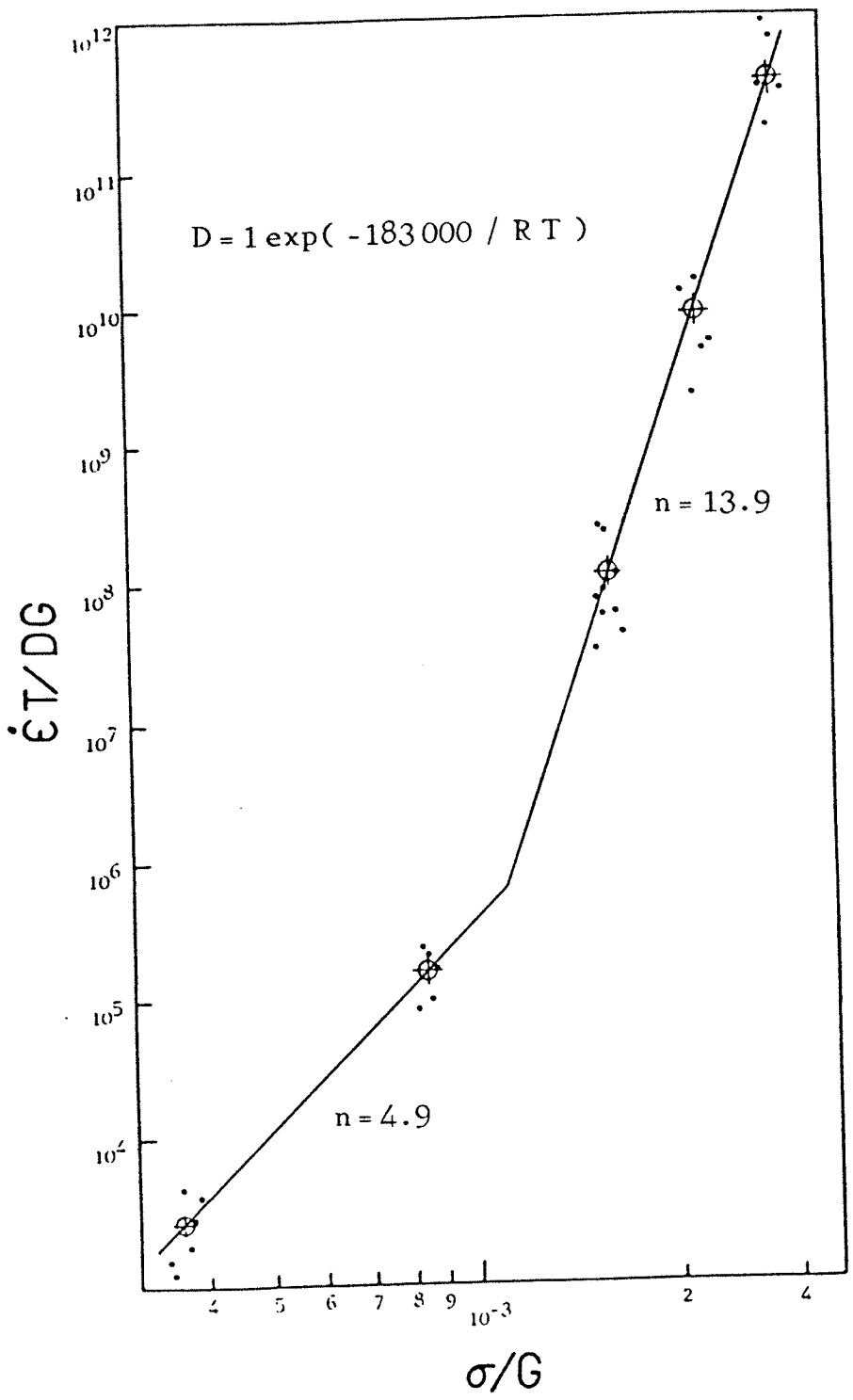

Figure 13: Stress dependence in region where Q for creep is high.

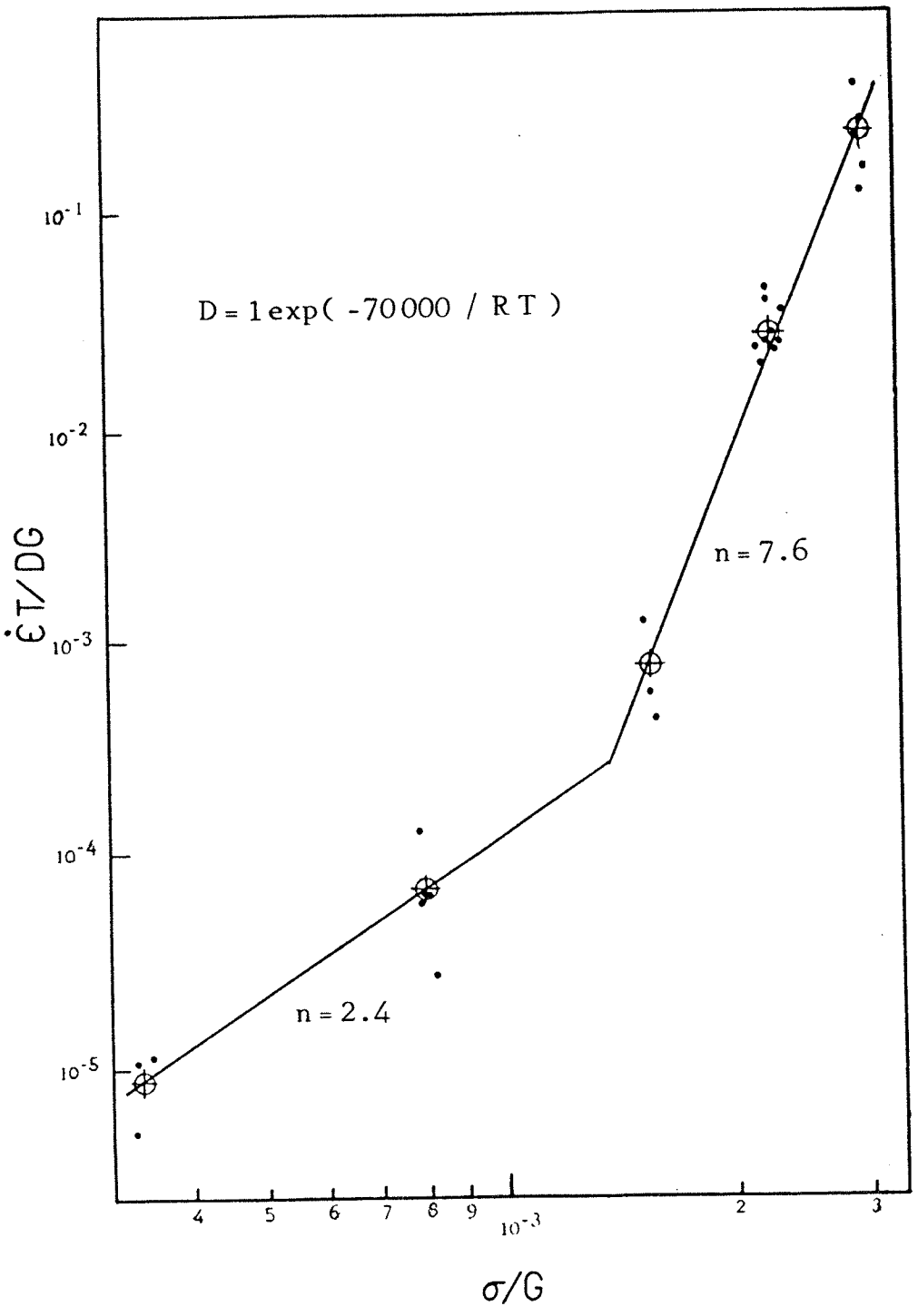

Figure 14: Stress dependence in region where Q for creep is low.

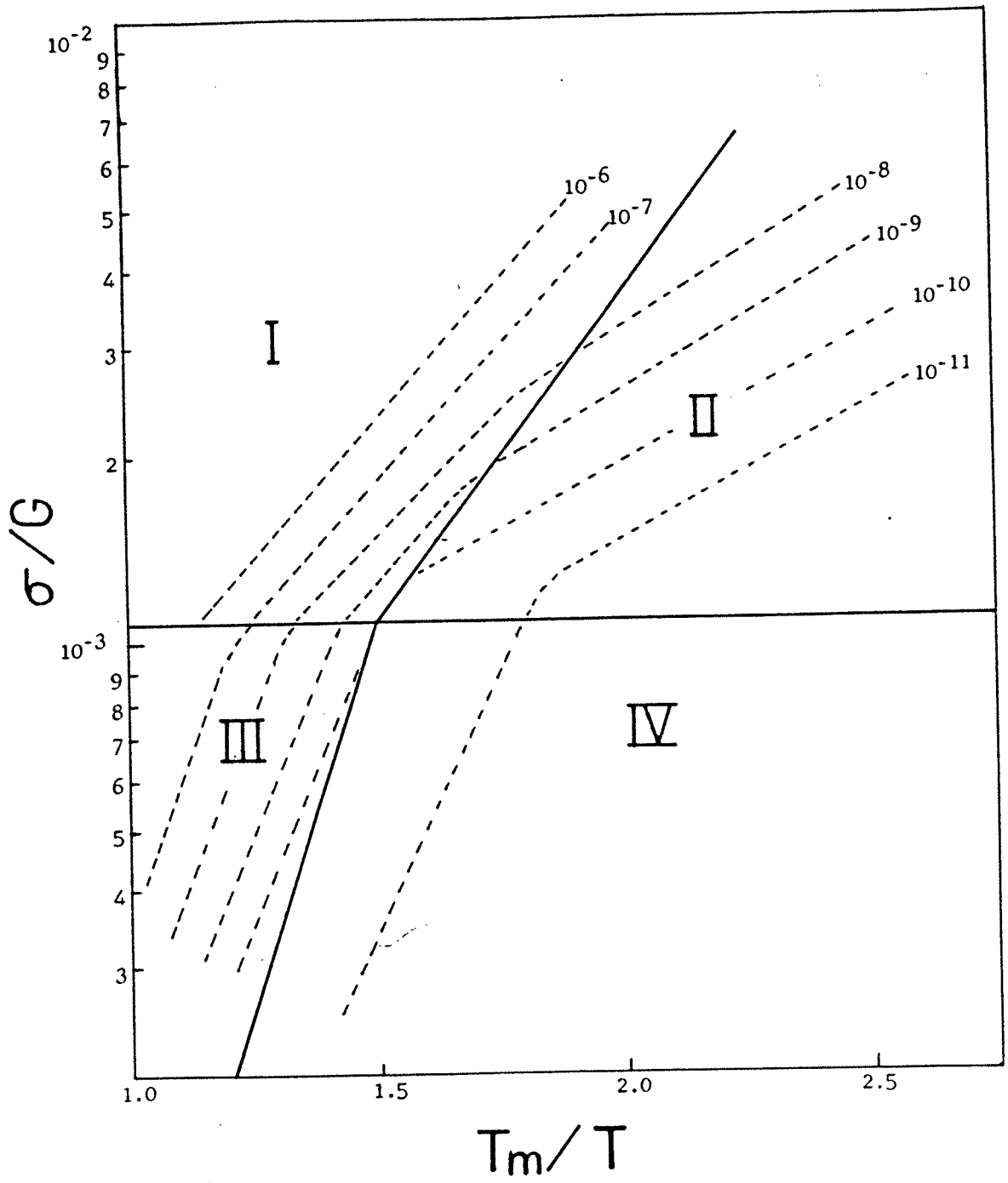

Figure 15: Deformation map for composite. Dashed lines represent lines of constant strain rate $\dot{\epsilon}T/G$.

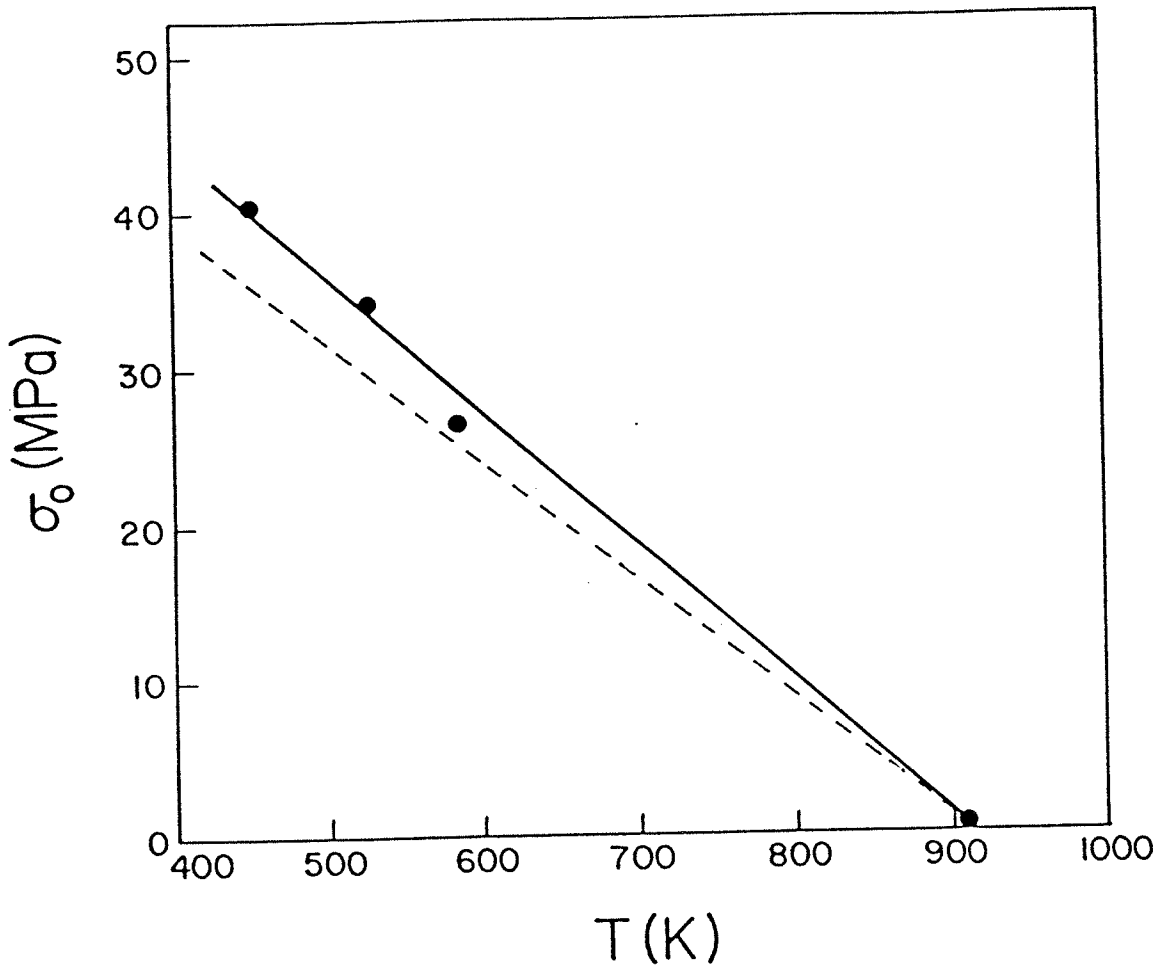

Figure 16: Threshold stress for Al-Ni eutectic. Dashed line represents values used for the calculation of stress exponents and activation energies.

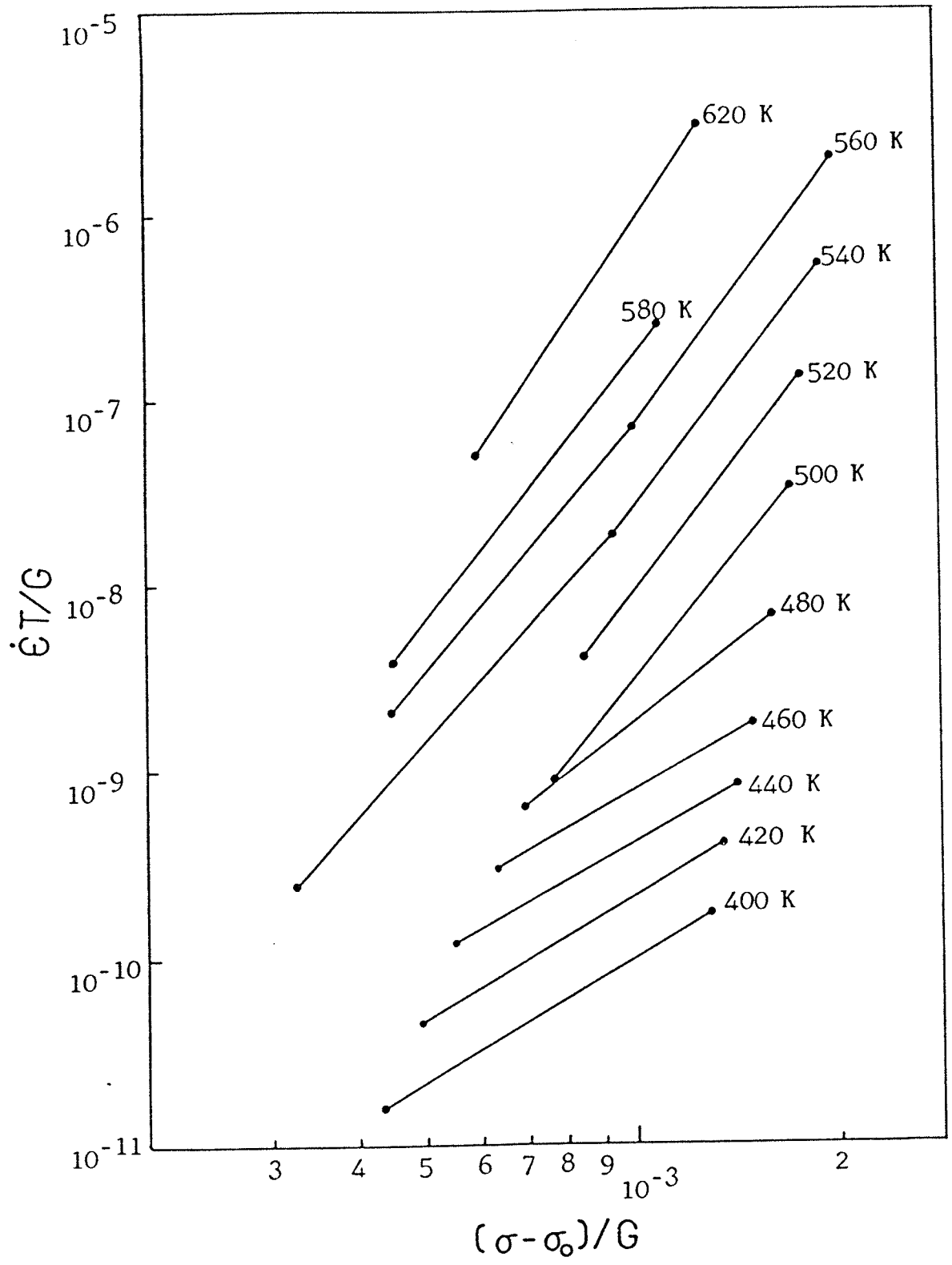

Figure 17: Determination of stress exponent with inclusion of σ_0

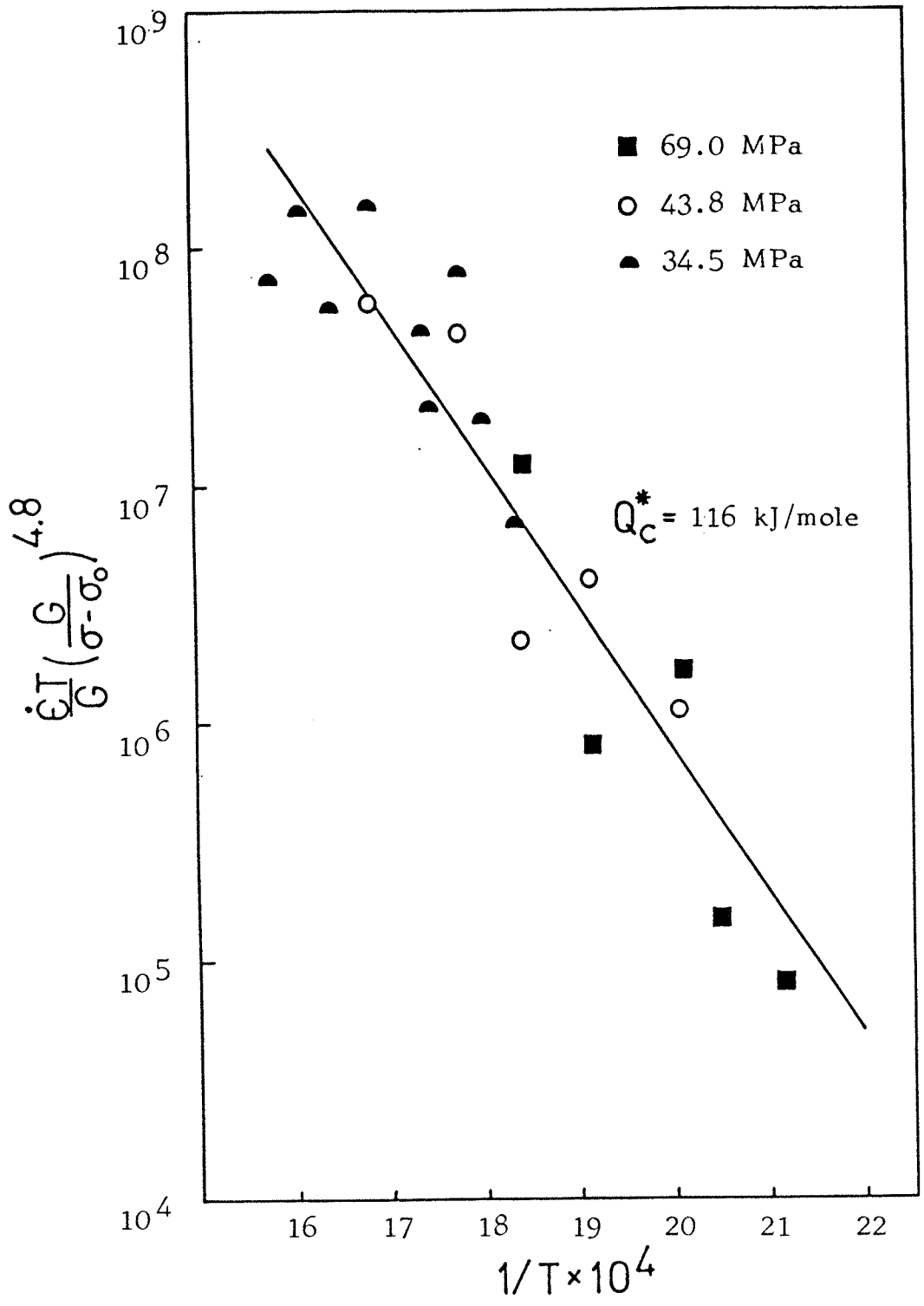

Figure 18: Creep activation energy with inclusion of σ_o for n_o= 4.8.

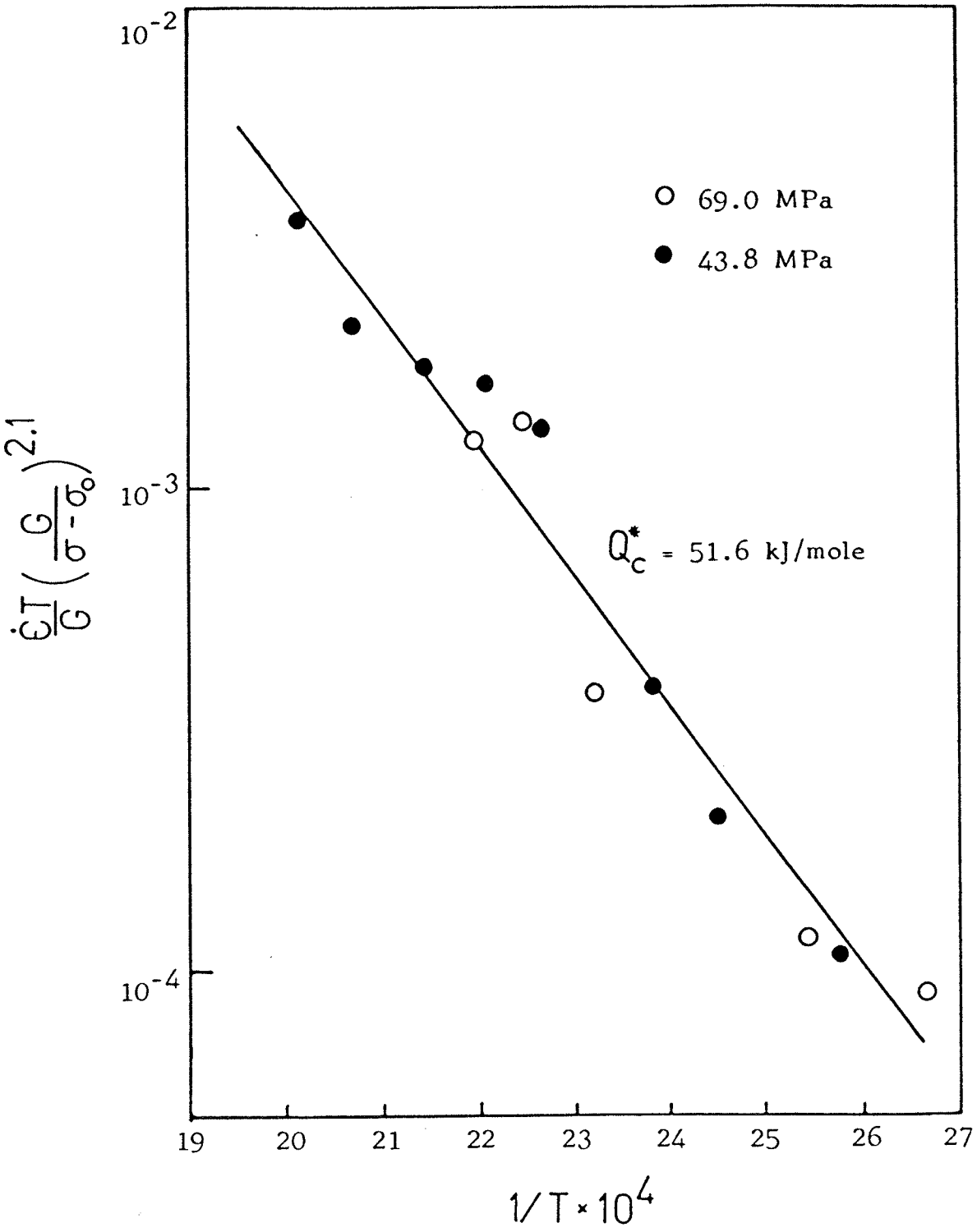

Figure 19: Creep activation energy with inclusion of σ_o for n_o= 2.1.

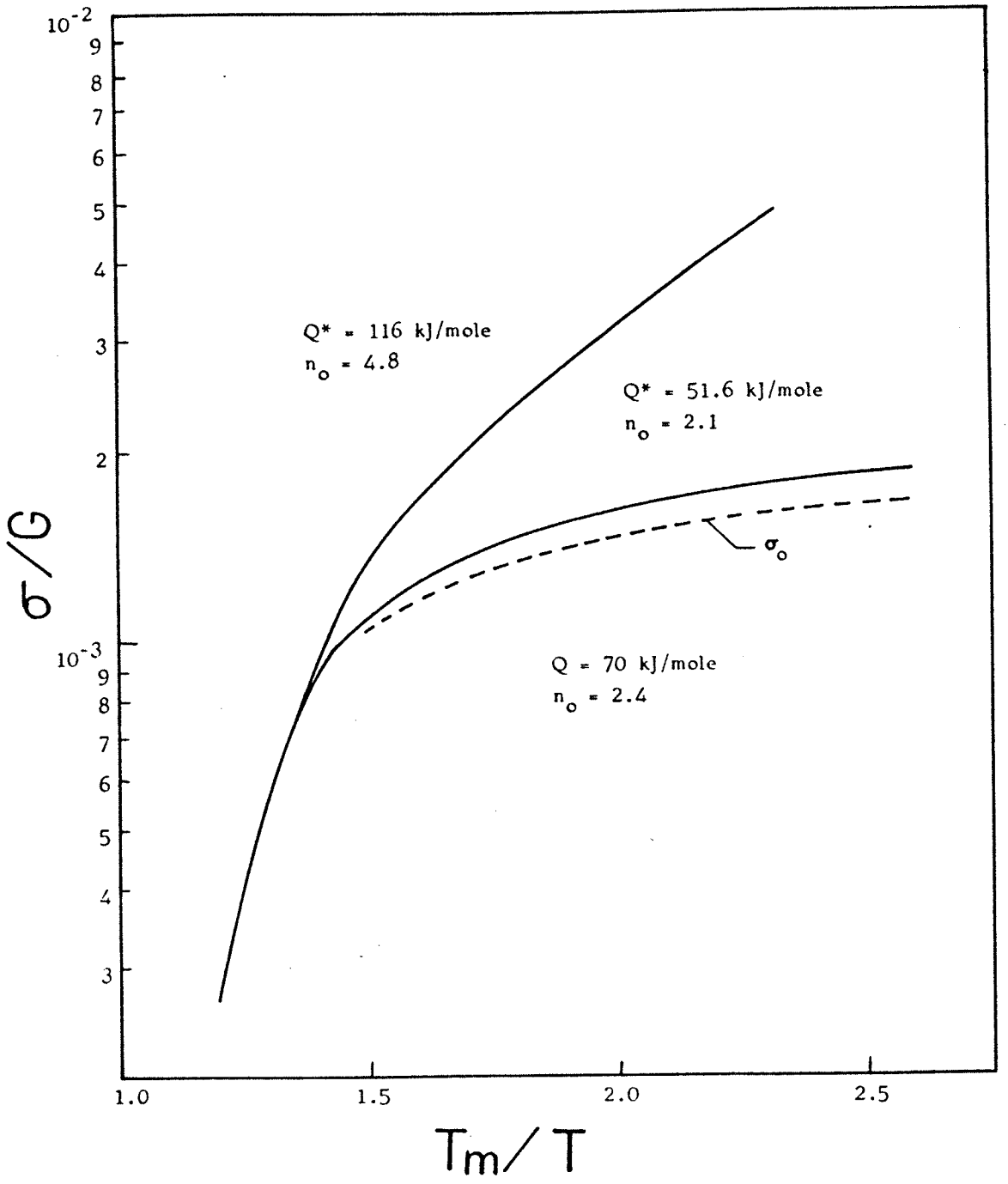

Figure 20: New deformation map for composite assuming a threshold stress.

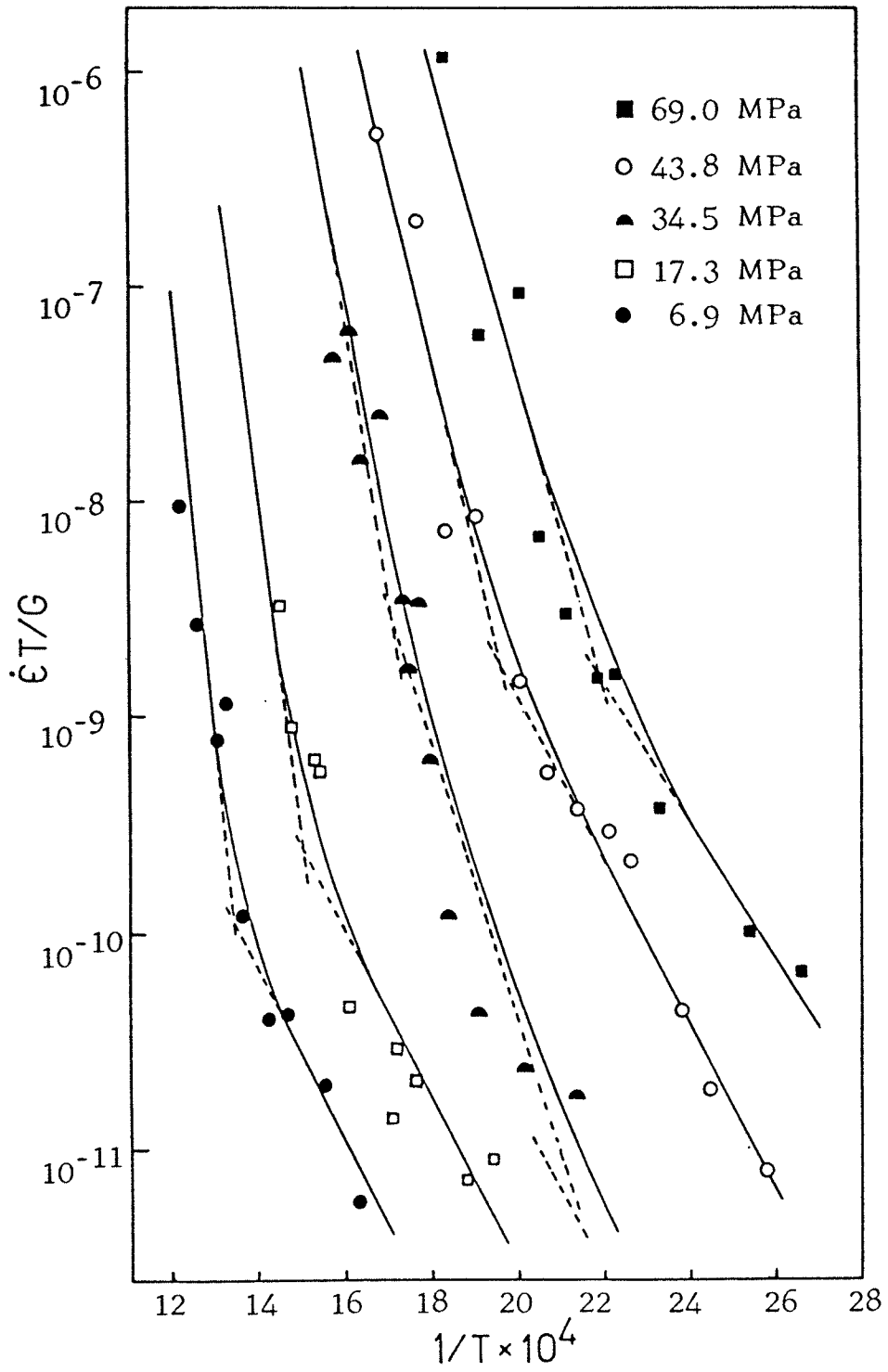

Figure 21: Comparison of equations 1,2 and 3 with the creep data. Solid lines represent the sum of the individual mechanisms shown by the dashed lines.

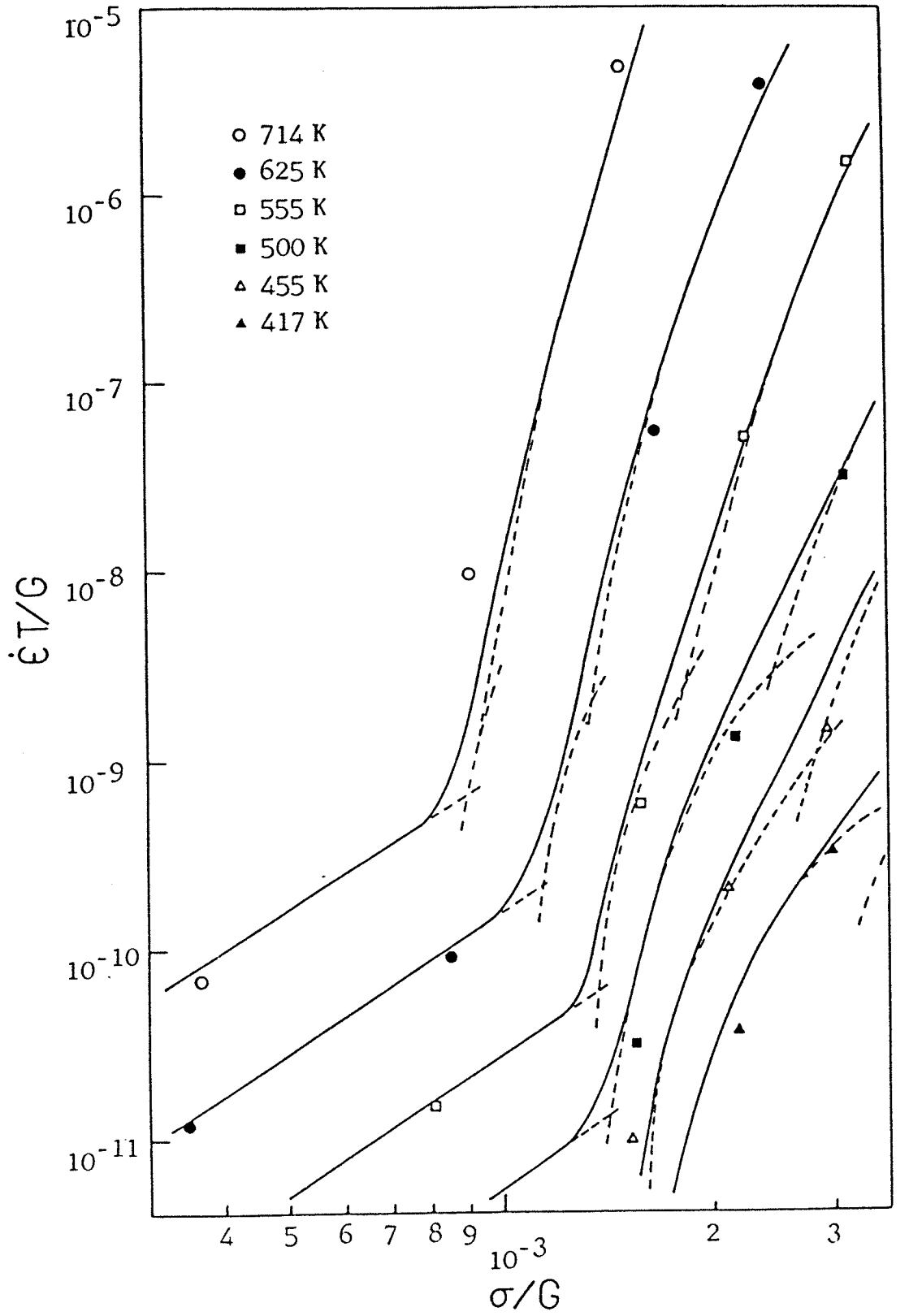

Figure 22: Comparison of equations 1, 2 and 3 with creep data. Solid lines represent the sum of the individual mechanisms shown by the dashed lines.

Figure 23: SEM Micrograph of fractured fibers in crept composite. (4000X)